TABLE 4 (Continued)

	English		Japanese			English		Japanese	
4	16	1.83	4	1.10	4	38	4.34	19	5.21
999	6	0.68	2	0.55	999	2	0.23	3	0.82
Total	876	100	365	100.00	Total	876	100	365	100.00
Rigidity, RUE*	Frequency	%	Frequency	%	Postural stability*	Frequency	%	Frequency	%
0	176	20.09	93	25.48	0	422	48.17	150	41.10
1	282	32.19	142	38.90	1	157	17.92	66	18.08
2	342	39.04	111	30.41	2	60	6.85	44	12.05
3	69	7.88	14	3.84	3	149	17.01	84	23.01
4	6	0.68	2	0.55	4	86	9.82	20	5.48
999	1	0.11	3	0.82	999	2	0.23	1	0.27
Total	876	100	365	100.00	Total	876	100	365	100.00
Rigidity, LUE*	Frequency	%	Frequency	%	Posture	Frequency	%	Frequency	%
0	205	23.4	99	27.12	0	173	19.75	78	21.37
1	268	30.59	135	36.99	1	337	38.47	129	35.34
2	317	36.19	121	33.15	2	206	23.52	84	23.01
3	77	8.79	9	2.47	3	125	14.27	52	14.25
4	7	0.8	1	0.27	4	33	3.77	21	5.75
999	2	0.23	0	0.00	999	2	0.23	1	0.27
Total	876	100	365	100.00	Total	876	100	365	100.00
Rigidity, RLE	Frequency	%	Frequency	%	Global spontaneity of movement	Frequency	%	Frequency	%
0	272	31.05	109	29.86	0	108	12.33	49	13.42
1	248	28.31	125	34.25	1	278	31.74	155	42.47
2	275	31.39	106	29.04	2	279	31.85	97	26.58
3	67	7.65	23	6.30	3	184	21	51	13.97
4	10	1.14	1	0.27	4	27	3.08	12	3.29
999	4	0.46	1	0.27	999	0	0	1	0.27
Total	876	100	365	100.00	Total	876	100	365	100.00
Rigidity, LLE	Frequency	%	Frequency	%	Postural tremor, right hand	Frequency	%	Frequency	%
0	286	32.65	116	31.78	0	544	62.1	223	61.10
1	227	25.91	120	32.88	1	262	29.91	119	32.60
2	275	31.39	100	27.40	2	43	4.91	19	5.21
3	75	8.56	26	7.12	3	23	2.63	2	0.55
4	11	1.26	1	0.27	4	1	0.11	2	0.55
999	2	0.23	2	0.55	999	3	0.34	0	0.00
Total	876	100	365	100.00	Total	876	100	365	100.00
Finger tapping, right hand*	Frequency	%	Frequency	%	Postural tremor, left hand*	Frequency	%	Frequency	%
0	122	13.93	95	26.03	0	518	59.13	234	64.11
1	342	39.04	167	45.75	1	276	31.51	98	26.85
2	252	28.77	64	17.53	2	49	5.59	27	7.40
3	144	16.44	35	9.59	3	29	3.31	2	0.55
4	15	1.71	3	0.82	4	1	0.11	1	0.27
999	1	0.11	1	0.27	999	3	0.34	3	0.82
Total	876	100	365	100.00	Total	876	100	365	100.00
Finger tapping, left hand*	Frequency	%	Frequency	%	Kinetic tremor, right hand*	Frequency	%	Frequency	%
0	108	12.33	91	24.93	0	546	62.33	258	70.68
1	298	34.02	135	36.99	1	265	30.25	89	24.38
2	265	30.25	96	26.30	2	46	5.25	15	4.11
3	181	20.66	37	10.14	3	13	1.48	1	0.27
4	22	2.51	5	1.37	4	2	0.23	1	0.27
999	2	0.23	1	0.27	999	4	0.46	1	0.27
Total	876	100	365	100.00	Total	876	100	365	100.00
Hand movements, right hand*	Frequency	%	Frequency	%	Kinetic tremor, left hand*	Frequency	%	Frequency	%
0	187	21.35	129	35.34	0	493	56.28	236	64.66
1	346	39.5	160	43.84	1	293	33.45	105	28.77
2	231	26.37	57	15.62	2	72	8.22	22	6.03
3	98	11.19	17	4.66	3	14	1.6	1	0.27
4	12	1.37	2	0.55	4	0	0	1	0.27
999	2	0.23	0	0.00	999	4	0.46	0	0.00
Total	876	100	365	100.00	Total	876	100	365	100.00
Hand movements, left hand*	Frequency	%	Frequency	%	Rest tremor amplitude, RUE*	Frequency	%	Frequency	%
0	164	18.72	118	32.33	0	586	66.89	281	76.99
1	311	35.5	147	40.27	1	112	12.79	51	13.97
2	250	28.54	78	21.37	2	121	13.81	26	7.12
3	125	14.27	17	4.66	3	53	6.05	6	1.64

doi:10.1002/mdc3.12058

TABLE 4 (Continued)

	English		Japanese			English		Japanese	
4	25	2.85	4	1.10	4	3	0.34	1	0.27
999	1	0.11	1	0.27	999	1	0.11	0	0.00
Total	876	100	365	100.00	Total	876	100	365	100.00
Pronation: supination movements, right hand*	Frequency	%	Frequency	%	Rest tremor amplitude, LUE*	Frequency	%	Frequency	%
0	199	22.72	100	27.40	0	603	68.84	280	76.71
1	335	38.24	159	43.56	1	120	13.7	56	15.34
2	216	24.66	64	17.53	2	99	11.3	20	5.48
3	107	12.21	35	9.59	3	45	5.14	9	2.47
4	17	1.94	6	1.64	4	5	0.57	0	0.00
999	2	0.23	1	0.27	999	4	0.46	0	0.00
Total	876	100	365	100.00	Total	876	100	365	100.00
Pronation: supination movements, left hand	Frequency	%	Frequency	%	Rest tremor amplitude, RLE	Frequency	%	Frequency	%
0	162	18.49	76	20.82	0	777	88.7	319	87.40
1	297	33.9	138	37.81	1	52	5.94	25	6.85
2	235	26.83	101	27.67	2	35	4	18	4.93
3	150	17.12	42	11.51	3	9	1.03	2	0.55
4	29	3.31	8	2.19	4	0	0	0	0.00
999	3	0.34	0	0.00	999	3	0.34	1	0.27
Total	876	100	365	100.00	Total	876	100	365	100.00
Toe tapping, right foot*	Frequency	%	Frequency	%	Rest tremor amplitude, LLE	Frequency	%	Frequency	%
0	168	19.18	89	24.38	0	795	90.75	319	87.40
1	323	36.87	149	40.82	1	46	5.25	24	6.58
2	228	26.03	96	26.30	2	20	2.28	17	4.66
3	129	14.73	24	6.58	3	12	1.37	2	0.55
4	27	3.08	6	1.64	4	0	0	0	0.00
999	1	0.11	1	0.27	999	3	0.34	3	0.82
Total	876	100	365	100.00	Total	876	100	365	100.00
Toe tapping, left foot*	Frequency	%	Frequency	%	Rest tremor amplitude, lip/jaw*	Frequency	%	Frequency	%
0	154	17.58	68	18.63	0	780	89.04	349	95.62
1	251	28.65	140	38.36	1	63	7.19	12	3.29
2	268	30.59	111	30.41	2	18	2.05	3	0.82
3	154	17.58	36	9.86	3	13	1.48	0	0.00
4	46	5.25	10	2.74	4	1	0.11	1	0.27
999	3	0.34	0	0.00	999	1	0.11	0	0.00
Total	876	100	365	100.00	Total	876	100	365	100.00
Leg agility, right leg*	Frequency	%	Frequency	%	Constancy of rest*	Frequency	%	Frequency	%
0	250	28.54	119	32.60	0	409	46.69	219	60.00
1	329	37.56	163	44.66	1	214	24.43	79	21.64
2	190	21.69	61	16.71	2	91	10.39	28	7.67
3	86	9.82	18	4.93	3	85	9.7	21	5.75
4	18	2.05	4	1.10	4	67	7.65	17	4.66
999	3	0.34	0	0.00	999	10	1.14	1	0.27
Total	876	100	365	100.00	Total	876	100	365	100.00
Leg agility, left leg*	Frequency	%	Frequency	%					
0	216	24.66	99	27.12					
1	298	34.02	142	38.90					
2	213	24.32	90	24.66					
3	106	12.1	30	8.22					
4	38	4.34	3	0.82					
999	5	0.57	1	0.27					
Total	876	100	365	100.00					
Part IV									
Time spent with dyskinesias*	Frequency	%	Frequency	%	Functional impact of fluctuations	Frequency	%	Frequency	%
0	563	64.27	273	74.79	0	433	49.43	194	53.15
1	173	19.75	41	11.23	1	165	18.84	56	15.34
2	87	9.93	30	8.22	2	81	9.25	32	8.77
3	27	3.08	12	3.29	3	119	13.58	60	16.44
4	17	1.94	6	1.64	4	63	7.19	19	5.21
999	9	1.03	3	0.82	999	15	1.71	4	1.10
Total	876	100	365	100.00	Total	876	100	365	100.00

doi:10.1002/mdc3.12058

TABLE 4 (Continued)

	English		Japanese			English		Japanese	
Functional impact of dyskinesias*	Frequency	%	Frequency	%	Complexity of motor fluctuations*	Frequency	%	Frequency	%
0	695	79.34	308	84.38	0	404	46.12	192	52.60
1	90	10.27	27	7.40	1	291	33.22	125	34.25
2	29	3.31	19	5.21	2	69	7.88	21	5.75
3	46	5.25	7	1.92	3	50	5.71	17	4.66
4	5	0.57	2	0.55	4	46	5.25	3	0.82
999	11	1.26	2	0.55	999	16	1.83	7	1.92
Total	876	100	365	100.00	Total	876	100	365	100.00
Time spent in the OFF state*	Frequency	%	Frequency	%	Painful OFF state dystonia*	Frequency	%	Frequency	%
0	383	43.72	183	50.14	0	680	77.63	319	87.40
1	341	38.93	113	30.96	1	114	13.01	28	7.67
2	106	12.1	50	13.70	2	45	5.14	4	1.10
3	22	2.51	14	3.84	3	13	1.48	6	1.64
4	14	1.6	2	0.55	4	15	1.71	5	1.37
999	10	1.14	3	0.82	999	9	1.03	3	0.82
Total	876	100	365	100.00	Total	876	100	365	100.00

[a]999 = missing.
*$P < 0.05$ by chi-square test (df = 4).
DDS, dopamine dysregulation syndrome; RUE, right upper extremity; LUE, left upper extremity; RLE, right lower extremity; LLE, left lower extremity.

Author Roles

(1) Research Project: A. Conception, B. Organization, C. Execution; (2) Statistical Analysis: A. Design, B. Execution, C. Review and Critique; (3) Manuscript: A. Writing of the First Draft, B. Review and Critique.

K. Kashihara: 1A, 1B, 1C, 2C, 3A, 3B
T. Kondo: 1A, 1B, 1C, 3A, 3B
Y. Mizuno: 1A, 1B, 1C, 3A, 3B
S. Kikuchi: 1B, 1C, 3B
S. Kuno: 1B, 1C, 3B
K. Hasegawa: 1B, 1C, 3A, 3B
N. Hattori: 1B, 1C, 3B
H. Mochizuki: 1B, 1C, 3B
H. Mori: 1B, 1C, 3B
M. Murata: 1B, 1C, 3B
M. Nomoto: 1B, 1C, 3B
R. Takahashi: 1B, 1C, 3B
A. Takeda: 1B, 1C, 3B
Y. Tsuboi: 1B, 1C, 3B
Y. Ugawa: 1B, 1C, 3B
M. Yamamoto: 1B, 1C, 3B
F. Yokochi: 1B, 1C, 3B
F. Yoshii: 1A, 1B, 1C, 3A, 3B
G.T. Stebbins: 1A, 1B, 1C, 2A, 2C, 3B
B.C. Tilley: 2C, 3B
L. Wang: 2B, 2C, 3A, 3B
S. Luo: 2C, 3B
N.R. LaPelle: 2A, 2B, 3B
C.G. Goetz: 1A, 1B, 1C, 2A, 2C, 3A, 3B

Disclosures

Funding Sources and Conflicts of Interest: This work was supported by Boehringer Ingelheim Japan. The administrative core members (G.T.S., B.C.T., S.L., L.W., N.R.L., and C.G.G.) were supported by funds from the Movement Disorder Society.

Financial Disclosures for previous 12 months: Kenichi Kashihara has served on the advisory board of Kyowa Hakko Kirin Co.; has been supported by Health and Labor Sciences Research Grants; has received honoraria from Boehringer Ingelheim, GlaxoSmithKline (GSK), Kyowa Hakko Kirin Co., Novartis, Otsuka Pharmaceutical Co., Dainippon Sumitomo Pharm Co., Ltd., and Fujimoto Pharmaceutical (FP) Pharmaceutical Co.; and has received royalties from Nankodo. Tomoyoshi Kondo has worked as a consultant for Kyowa Hakko Kirin Co. and Novartis and has received honoraria from Boeringer Ingelheim, GSK, Kyowa Hakko Kirin Co., Novartis, Otsuka Pharmaceutical Co., Dainippon Sumitomo Pharm Co., Ltd., and FP Pharmaceutical Co. Yoshikuni Mizuno has held advisory board membership with FP Pharmaceutical Co., Otsuka Pharmaceutical Co., AbbVie Japan, and Kyowa Hakko Kirin Co. and received personal compensation when he attended advisory board meetings and has been supported by grants from Boehringer Ingelheim. Seiji Kikuchi has been supported by grants from the Ministry of Health, Labor and Welfare of Japan and has received honoraria from Boehringer Ingelheim, GSK, Kyowa Hakko Kirin Co., Novartis, Otsuka Pharmaceutical Co., Dainippon Sumitomo Pharm Co., Ltd., FP Pharmaceutical Co., Daiichi-Sankyo, Takeda Pharmaceutical Co., Biogen Idec Japan, Bayer Yakuhin, Genzyme Japan, Nihon Pharmaceutical Co., and Mitsubishi Tanabe Pharma. Sadako Kuno has served on the advisory board of AbbVie Japan and has received honoraria from Boehringer Ingelheim, GSK, Kyowa Hakko Kirin Co., Novartis, Otsuka Pharmaceutical Co., Dainippon Sumitomo Pharm Co., Ltd., FP Pharmaceutical Co., Ono Pharmaceutical Co., AbbVie Japan, and Alfresa Pharma. Kazuko Hasegawa has received honoraria from Boehringer Ingelheim, GSK, Kyowa Hakko Kirin Co., Novartis, Otsuka Pharmaceutical

doi:10.1002/mdc3.12058

Co., and Dainippon Sumitomo Pharm Co., Ltd. Nobutaka Hattori has worked as a consultant for Hisamitsu Pharmaceutical; has been supported by grants from Otsuka Pharmaceutical, Boehringer Ingelheim, and Kyowa Hakko-Kirin Pharmaceutical Company; and has received honoraria from GSK K.K., Nippon Boehringer Ingelheim, Co., Ltd., FP Pharmaceutical Co., Otsuka Pharmaceutical, Co., Ltd., Dainippon Sumitomo Pharma Co., Ltd., Novartis Pharma K.K., Eisai Co., Ltd., Medtronic, Inc., Kissei Pharmaceutical Company, Janssen Pharmaceutical K.K., Nihon Medi-Physics Co., Ltd., Astellas Pharma Inc., and Kyowa Hakko-Kirin Co., Ltd. Hideki Mochizuki has been supported by grants from Grant-in-Aid for Scientific Research from the Ministry of Education, Culture, Sports, Science and Technology of Japan, Grant-in-Aid for JST-CREST Basic Research Program from the Ministry of Education, Culture, Sports, Science and Technology of Japan, Grant-in-Aid for Scientific Research on Innovative Areas (Brain Environment) from the Ministry of Education, Science, Sports and Culture of Japan, and Grant-in-Aid for Research on Applying Health Technology from the Ministry of Health, Labor and Welfare of Japan; has received honoraria from Biogen Idec Japan, Eisai Co., Ltd., FP Pharmaceutical Co., Elsevier Japan, Hisamitsu Pharma, Kyowa Hakko Kirin Co., GSK, Dainippon Sumitomo Pharm Co., Ltd., FP Pharmaceutical Co., Takeda Pharmaceutical Co., Mitsubishi Tanabe Pharma, Nippon Chemiphar Co., Nihon Medi-Physics Co., Boehringer Ingelheim, Novartis, and UCB Japan; and has received royalties from Nature Japan, Igaku-Shoin, Iyaku Journal, Nanzando Co., and Kinpodo. Hideo Mori has received honoraria from Boehringer Ingelheim, GSK, Otsuka Pharmaceutical Co., Dainippon Sumitomo Pharm Co., Ltd., and FP Pharmaceutical Co. Miho Murata has been supported by grants from the Ministry of Health, Labor and Welfare of Japan and has received honoraria from Boehringer Ingelheim, GSK, Kyowa Hakko Kirin Co., Novartis, Otsuka Pharmaceutical Co., Dainippon Sumitomo Pharm Co., Ltd., and Nihon Medi-Physics Co. Masahiro Nomoto has been awarded grants and research support from the Ministry of Health, Labor and Welfare of Japan, Dainippon Sumitomo Pharm Co., Ltd., Boehringer Ingelheim, Novartis, GSK, FP Pharmaceutical Co., Genzyme, and Tsumura & Co.; has worked as a consultant for and held advisory board membership with honoraria with the Japanese Society of Internal Medicine, Takeda Pharm Co., FP Pharmaceutical Co., Kyowa Hakko Kirin Co., Otsuka Pharm Co., Hisamitsu, Ono Pharm Co., and Meiji Seika; has received honoraria from Boehringer Ingelheim, GSK, Dainippon Sumitomo Pharm Co., Ltd., FP Pharmaceutical Co., Novartis, Kyowa Hakko Kirin Co., Otsuka Pharm Co., Genzyme, Panasonic Healthcare Co., and UCB Inc.; and has received royalties from Maruzen, Igaku-Shoin, and Nishimura. Ryosuke Takahashi has worked as a consultant for KAN Research Institute, Inc., and Daiichi-Sankyo; has been awarded grants and research support from Dainippon Sumitomo Pharm Co., Ltd., Boehringer Ingelheim, Novartis, Pfizer Co., Ltd., GSK, Takeda Pharmaceutical Co., Mitsubishi Tanabe Pharma, and Kyowa Hakko Kirin Co.; and has received honoraria from Boehringer Ingelheim, GSK, Dainippon Sumitomo Pharm Co., Ltd., FP Pharmaceutical Co., Medical Review, Novartis, Daiichi-Sankyo, Kyowa Hakko Kirin Co., Mitsubishi Tanabe Pharma, Eisai Co., Ltd., Nihon Pharmaceutical Co., Otsuka Pharmaceutical Co., Janssen Pharmaceutical Company, Sanofi, Alfresa Pharma Co., Japan Blood Products Organization, Asbio Pharma Co., Ltd., and MSD. Atsushi Takeda has been supported by grants from the Ministry of Education, Culture, Sports, Science and Technology of Japan and the Ministry of Health, Labor and Welfare of Japan; has received honoraria from Otsuka Pharmaceutical Co., Kyowa Hakko Kirin Co., Ltd., GSK, Daiichi-Sankyo, Dainippon Sumitomo Pharm Co., Ltd., FP Pharmaceutical Co., Takeda Pharmaceutical Co., Boehringer Ingelheim, Novartis, and Ono Pharmaceutical; and has received royalties from Iyaku Journal, Chugai-Igakusha, Igaku-Shoin, Medical View, Elsevier Japan, and Aruta Shuppan. Yoshio Tsuboi has been supported by grants from the Ministry of Health, Labor and Welfare of Japan and has received honoraria from Eisai Co., Ltd., Otsuka Pharmaceutical Co., Kyowa Hakko Kirin Co., GSK, Daiichi-Sankyo, Dainippon Sumitomo Pharm Co., Ltd., FP Pharmaceutical Co., Mitsubishi Tanabe Pharma, Teijin Pharma, Boehringer Ingelheim, and Novartis. Yoshikazu Ugawa has been supported by grants from the Ministry of Education, Culture, Sports, Science and Technology of Japan, the Ministry of Health, Labor and Welfare of Japan, the Support Center for Advanced Telecommunications Technology Research, the Association of Radio Industries Businesses, the Uehara Memorial Foundation, Novartis Foundation (Japan) for the Promotion of Science, JST, and Nihon Kohden; has received honoraria from the Taiwan Society of Clinical Neurophysiology, Indonesia Society of Clinical Neurophysiology, Taiwan Movement Disorders Society, Astellas Pharma, Eisai Co. Ltd., Dainippon Sumitomo Pharm Co., Ltd., FP Pharmaceutical Co., Otsuka Pharmaceutical Co., Elsevier Japan, Kissei Pharmaceutical Co., Kyorin Pharma, Kyowa Hakko Kirin Co., GSK, Sanofi, Daiichi-Sankyo, Takeda Pharmaceutical Co., Mitsubishi Tanebe Pharma, Teijin Pharma, Nippon Chemiphar Co., Nihon Pharmaceutical Co., Boehringer Ingelheim, Novartis, Bayer Yakuhin, and Mochida Pharma; and has received royalties from Chugai-Igakusha, Igaku-Shoin Ltd., Medical View, and Blackwell Publishing. Mitsutoshi Yamamoto has received honoraria from Dainippon Sumitomo Pharm Co., Ltd., Boehringer Ingelheim, Novartis, GSK, FP Pharmaceutical Co., Kyowa Hakko Kirin Co., and Otsuka Pharm Co. Fusako Yokochi has received honoraria from GSK, Otsuka Pharmaceutical Co., Medtronic, and AbbVie Japan. Fumihito Yoshii has been supported by grants from Eisai Co., Ltd., Dainippon Sumitomo Pharm Co., Ltd., FP Pharmaceutical Co., Takeda Pharmaceutical Co., Mitsubishi Tanabe Pharma, GSK, Boehringer Ingelheim, Daiichi-Sankyo, Mitsubishi Tanabe Pharma, and Pfizer and has received honoraria from GSK, Dainippon Sumitomo Pharm Co., Ltd., Boehringer Ingelheim, Novartis, AbbVie Japan, Ono Parmaceutical Co., Otsuka Pharmaceutical Co., and Janssen Pharmaceutical Co. Glenn T. Stebbins has worked as a consultant for and held advisory board membership with honoraria with Adamas Pharmaceuticals, Inc., Ceregene, Inc., Child Health and Development Institute (CHDI) Management,

doi:10.1002/mdc3.12058

Inc., Ingenix Pharmaceutical Services (i3 Research), and Neurocrine Biosciences, Inc.; has been awarded grants and research support from the National Institutes of Health (NIH), the Michael J. Fox Foundation (MJFF) for Parkinson's Research, and the Dystonia Coalition; has received honoraria from the International Parkinson and Movement Disorder Society (MDS), American Academy of Neurology, and the MJFF; and has received a salary from Rush University Medical Center. Barbara C. Tilley has been awarded grants from the NIH (National Institute of Neurological Disorders and Stroke, National Heart, Lung and Blood Institute, National Institute on Minority Health and Health Disparities, and National Institute of General Medical Sciences), the Pfizer Data and Safety Monitoring Committee and the NIH Data and Safety Monitoring Committees and has received a salary from the University of Texas Health Science Center School of Public Health at Houston, Division of Biostatistics. Sheng Luo and Lu Wang have nothing to declare. Nancy R. Lapelle has worked in cognitive testing, qualitative research, and program/process evaluation consulting for the UMass Medical School (UMMS) Lamar Soutter Library, UMass Medical School Inter-Professional Development, The Association of Academic Health Sciences Libraries, Medical University of South Carolina (MUSC) College of Nursing and Hollings Cancer Center, and the MDS; Dr. Lapelle is a subcontractor on a variety of research and evaluation grants with principal investigators at UMMS and MUSC. Christopher G. Goetz has worked as a consultant for and held advisory board membership with honoraria with AOP Orphan, Addex Pharma, Advanced Studies of Medicine, Boston Scientific, CHDI, Health Advances, ICON Clinical Research, Inc., Ingenix (i3 Research), the NIH, Neurocrine, Oxford Biomedica, and Synthonics and has been awarded grants and research support with funding from the NIH and the MJFF. Dr. Goetz directs the Rush Parkinson's Disease Research Center that receives support from the Parkinson's Disease Foundation; he directs the translation program for the MDS-UPDRS and UDysRS and receives funds from the MDS for this effort; has received honoraria from the MDS, the American Academy of Neurology, University of Pennsylvania, University of Chicago, and University of Luxembourg; has received royalties from Oxford University Press, Elsevier Publishers, and Wolters Kluwer Health–Lippincott, Wilkins and Williams; and has received a salary from Rush University Medical Center.

APPENDIX The MDS-UPDRS Japanese Validation Study Group

Investigators	Affiliation
Takashi Abe, MD	Department of Neurology, Abe Neurological Clinic
Kenichi Fujimoto, MD	Department of Neurology, Jichi Medical University Hospital
Kazuko Hasegawa, MD	Department of Neurology, National Sagamihara Hospital
Nobutaka Hattori, MD	Department of Neurology, Juntendo University School of Medicine
Yasuto Higashi, MD	Department of Neurology, Himeji Central Hospital
Takaki Imamura, MD	Department of Neurology, Okayama Kyokuto Hospital
Hidehumi Ito, MD	Department of Neurology, Wakayama Medical University
Kazunori Ito, MD	Department of Neurology, Iwamizawa Neurological Medical Clinic
Kenichi Kashihara, MD	Department of Neurology, Okayama Kyokuto Hospital
Jyunya Kawada, MD	Department of Neurology, Shonan Kamakura General Hospital
Noriko Kawashima, MD	Department of Neurology, Kawashima Neurology Clinic
Seiji Kikuchi, MD	National Hospital Organization Hokkaido Medical Center
Sadako Kuno, MD	Kyoto Shijyo Hospital
Tetsuya Maeda, MD	Department of Neurology, Research Institute for Brain and Blood Vessels-Akita
Hideki Mochizuki, MD	Department of Neurology, Osaka University Graduate School of Medicine
Hideo Mori, MD	Department of Neurology, Juntendo University Koshigaya Hospital
Kenya Murata, MD	Department of Neurology, Wakayama Medical University
Miho Murata, MD	Department of Neurology, National Center of Neurology and Psychiatry, Parkinson Disease and Movement Disorder Center
Masahiro Nomoto, MD	Department of Neurology and Clinical Pharmacology, Ehime University Graduate School of Medicine
Yasuyuki Okuma, MD	Juntendo University Shizuoka Hospital
Hidemoto Saiki, MD	Department of Neurology, Kitano Hospital
Hideyuki Sawada, MD	National Hospital Organization Utano Hospital
Ryosuke Takahashi, MD	Department of Neurology, Graduate School of Medicine, Kyoto University
Atsushi Takeda, MD	Department of Neurology, Tohoku University Medical School
Asako Takei, MD	Department of Neurology, Hokuyukai Neurological Hospital
Yasuo Terayama, MD	Department of Neurology, Iwate Medical University
Masahiko Tomiyama, MD	Department of Neurology, Aomori Prefectural Central Hospital
Yoshio Tsuboi, MD	Department of Neurology, Fukuoka University Medical School
Yoshikazu Ugawa, MD	Department of Neurology, Fukushima Medical University
Mitsutoshi Yamamoto, MD	Takamatsu Neurology Clinic
Fusako Yokochi, MD	Department of Neurology, Tokyo Metropolitan Neurological Hospital
Kazuto Yoshida, MD	Department of Neurology, Japanese Red Cross Asahikawa Hospital
Fumihito Yoshii, MD	Department of Neurology, Tokai University School of Medicine

Investigators involved in the cognitive pretesting and/or validation and their affiliations.

doi:10.1002/mdc3.12058

References

1. Fahn S, Elton RL. Unified Parkinson's Disease Rating Scale. In: Fahn S, Marsden CD, Goldstein M, Calne DB, eds. *Recent Developments in Parkinson's Disease*, Vol. 2. Florham Park, NJ: MacMillan Healthcare Information; 1987:153–164.
2. Movement Disorder Society Task Force on Rating Scales for Parkinson's Disease. The Unified Parkinson's Disease Rating Scale (UPDRS): status and recommendations. *Mov Disord* 2003;18: 738–750.
3. Barone P, Antonini A, Colosimo C, et al. The PRIAMO study: a multicenter assessment of nonmotor symptoms and their impact on quality of life in Parkinson's disease. *Mov Disord* 2009;24:1641–1649.
4. Goetz CG, Tilley BC, Shaftman SR, et al. Movement Disorder Society-sponsored revision of the Unified Parkinson's Disease Rating Scale (MDS-UPDRS): scale presentation and clinimetric testing results. *Mov Disord* 2008;23:2129–2170.
5. Antonini A, Abbruzzese G, Ferini-Strambi L, et al. Validation of the Italian version of the Movement Disorder Society-Unified Parkinson's Disease Rating Scale. *Neurol Sci* 2013;34:683–687.
6. Martinez-Martin P, Rodriguez-Blazquez C, Alvarez-Sanchez M, et al. Expanded and independent validation of the Movement Disorder Society-Unified Parkinson's Disease Rating Scale (MDS-UPDRS). *J Neurol* 2013;260:228–236.
7. Fowler FJ. *Improving Survey Questions*. Thousand Oaks, CA: Sage; 1995.
8. Hatcher L. *Step-by-Step Approach to Using the SAS System for Factor Analysis and Structural Equation Modeling*. Cary, NC: SAS Institute; 1994.
9. Muthen LK, Muthen BO. *M-plus User's Guide*. 6th ed. Los Angeles, CA: Muthen & Muthen; 2010.
10. Brown TA. *Confirmatory Factor Analysis for Applied Research*. New York, NY: Guilford SAGE Publications Inc; 2006.
11. Browne MW. An overview of analytic rotation in exploratory factor analysis. *Multivar Behav Res* 2001;36:111–150.
12. Gorsuch RL. *Factor Analysis*. 2nd ed. Hillsdale, NJ: Lawrence Erlbaum Associations Inc; 1983.
13. Forero CG, Maydeu-Olivares A, Gallardo-Pujol D. Factor analysis with ordinal indicators: a Monte Carlo study comparing DWLS and ULS estimation. *Struct Equ Model* 2009;16:625–641.
14. Kimura H, Kurimura M, Wada M, et al. Female preponderance of Parkinson's disease in Japan. *Neuroepidemiology* 2002;21:292–296.
15. Hely MA, Reid WG, Adena MA, et al. The Sydney multicenter study of Parkinson's disease: the inevitability of dementia at 20 years. *Mov Disord* 2008;23:837–844.
16. Morgante L, Colosimo C, Antonini A, et al. Psychosis associated to Parkinson's disease in the early stages: relevance of cognitive decline and depression. *J Neurol Neurosurg Psychiatry* 2012;83:76–82.

doi:10.1002/mdc3.12058

Neurobiology of Aging 35 (2014) 2656.e17–2656.e23

Contents lists available at ScienceDirect

Neurobiology of Aging

journal homepage: www.elsevier.com/locate/neuaging

Identification of a Japanese family with *LRRK2* p.R1441G-related Parkinson's disease

Taku Hatano [a,*], Manabu Funayama [a,b], Shin-ichiro Kubo [a], Ignacio F. Mata [d,e], Yutaka Oji [a], Akio Mori [a], Cyrus P. Zabetian [d,e], Sarah M. Waldherr [d,e], Hiroyo Yoshino [b], Genko Oyama [a], Yasushi Shimo [a,c], Ken-ichi Fujimoto [f], Hirokazu Oshima [g], Yasuto Kunii [g], Hirooki Yabe [g], Yoshikuni Mizuno [a], Nobutaka Hattori [a,b,*]

[a] *Department of Neurology, Juntendo University School of Medicine, Tokyo, Japan*
[b] *Research Institute for Diseases of Old Age, Juntendo University Graduate School of Medicine, Tokyo, Japan*
[c] *Department of Research and Therapeutics for Movement Disorders, Juntendo University School of Medicine, Tokyo, Japan*
[d] *Geriatric Research Education and Clinical Center, VA Puget Sound Health Care System, Seattle, WA, USA*
[e] *Department of Neurology, University of Washington, Seattle, WA, USA*
[f] *Jichi-idai Station Brain Clinic, Tochigi, Japan*
[g] *Department of Neuropsychiatry, Fukushima Medical University, Fukushima, Japan*

ARTICLE INFO

Article history:
Received 15 February 2014
Received in revised form 26 May 2014
Accepted 27 May 2014
Available online 2 June 2014

Keywords:
Parkinson's disease
LRRK2
p.R1441G
Asia
Intrafamilial clinical heterogeneity

ABSTRACT

Leucine-rich repeat kinase 2 (*LRRK2*) is a causative gene of autosomal dominant familial Parkinson's disease (PD). We screened for *LRRK2* mutations in 3 frequently reported exons (31, 41, and 48) in our cohort of 871 Japanese patients with PD (430 with sporadic PD and 441 probands with familial PD). Direct sequencing analysis of *LRRK2* revealed 1 proband (0.11%) with a p.R1441G mutation, identified for the first time in Asian countries, besides frequently reported substitutions including, the p.G2019S mutation (0.11%) and p.G2385R variant (11.37%). Several studies have suggested that the *LRRK2* p.R1441G mutation, which is highly prevalent in the Basque country, is extremely rare outside of northern Spain. Further analysis of family members of the proband with the p.R1441G mutation revealed that her mother and first cousin shared the same mutation and parkinsonism. Haplotype analysis revealed a different haplotype from that of the original Spanish families. Our patients demonstrated levodopa-responsive parkinsonism with intrafamilial clinical heterogeneity. This is the first report of familial PD because of the *LRRK2* p.R1441G mutation in Asia.

1. Introduction

Leucine-rich repeat kinase 2 (*LRRK2*) is one of the causative genes of autosomal dominant Parkinson's disease (PD) (Paisan-Ruiz et al., 2004; Zimprich et al., 2004). To date, 7 mutations in *LRRK2* p.G2019S, p.I2020T, p.N1437H, p.R1441G/C/H, and p.Y1699C have been proven as pathogenic mutations. Although p.G2019S and p.R1441G/C/H are frequent mutations in *LRRK2* and the prevalence of the p.G2019S mutation, the most common *LRRK2* substitution in populations of European origin, is estimated at 5%–13% of individuals with familial PD (Haugarvoll and Wszolek, 2009), the p.R1441C, p.R1441H, and p.G2019S mutations have been found to be very rare in Asia (Haugarvoll et al., 2008; Ross et al., 2009). The p.R1441G mutation is frequent in Spain, and especially in the Basque country, where it accounts for 16% of familial and 4% of sporadic cases (Haugarvoll and Wszolek, 2009). However, p.R1441G carriers are extremely rare outside of Spain (Haugarvoll and Wszolek, 2009; Mata et al., 2005, 2009b; Simon-Sanchez et al., 2006). To date, only 4 probands with p.R1441G outside of northern Spain have been reported (Cornejo-Olivas et al., 2013; Deng et al., 2006; Mata et al., 2009a; Yescas et al., 2010). Interestingly, most of the reported p.R1441G PD patients share a common founder, and this mutation is regarded as a rare haplotype (Haugarvoll and Wszolek, 2009; Mata et al., 2005, 2009b; Simon-Sanchez et al., 2006). It remains unclear whether there are patients carrying the p.R1441G mutation in Asia. In this study, we performed a mutation screening of exons 31, 41, and 48 of *LRRK2* in a Japanese cohort of PD patients and found a proband with the p.R1441G mutation. Here, we report the results of a

* Corresponding authors at: Department of Neurology, Juntendo University School of Medicine, 2-1-1 Hongo, Bunkyo-ku, Tokyo 113-8421, Japan. Tel.: +81 3 3813 3111; fax: +81 3 5800 0547.
E-mail addresses: thatano@juntendo.ac.jp (T. Hatano), nhattori@juntendo.ac.jp (N. Hattori).

0197-4580/$ – see front matter © 2014 Elsevier Inc. All rights reserved.
http://dx.doi.org/10.1016/j.neurobiolaging.2014.05.025

clinicoradiological and haplotype analysis of the first familial PD patients linked to p.R1441G mutation in Asian countries.

2. Methods

2.1. Subjects

We studied 871 Japanese PD patients (430 patients with sporadic PD and 441 probands with familial PD; age, 56.4 ± 14.5 years; age at onset, 49.8 ± 14.6 years; disease duration; 6.67 ± 6.89 years). A clinical diagnosis of PD was determined by the presence of at least 2 of 3 cardinal signs (rest tremor, bradykinesia, and rigidity) and improvement following adequate dopaminergic therapy (when available). In this study, families with 2 or more affected members or 2 members with a mutation in at least 2 generations were classified as autosomal dominant PD families, and families with at least 2 affected siblings in only 1 generation were classified as (potential or pseudo-) autosomal recessive PD families. Written informed consent was obtained from all participants, and the local ethics authorities approved the project. A 2-generation pedigree was established for the Japanese family with the *LRRK2* p.R1441G mutation (Fig. 1A). Among the 12 subjects in the family, 4 (II:5, II:4, I:6, and II:2) were willing to participate in this clinicogenetic study, whereas the remainder, including 2 reportedly parkinsonian subjects (I:2 and I:3), refused to participate. Participating individuals were examined by neurologists specializing in movement disorders. A full history was collected and a neurologic examination was performed for each patient.

2.2. Genetic analysis

Genomic DNA from each subject was extracted from peripheral blood using the QIAamp DNA Blood Maxi Kit (QIAGEN, Valencia, CA, USA). Three exons of *LRRK2* that have been frequently reported to contain PD-associated mutations (exons 31, 41, and 48) were analyzed by polymerase chain reaction-direct sequencing using the Big Dye Terminator v.1.1 Cycle Sequencing Kit (Life Technologies, Foster City, CA, USA) as previously described (Zimprich et al., 2004). Haplotype analysis of *LRRK2* flanking region was performed using previously described methods (Mata et al., 2005, 2009a, 2009b).

3. Results

3.1. Genetic findings

In this cohort, we identified 1 proband (0.11%) with a p.R1441G mutation, 1 with a p.G2019S mutation (0.11%), and 103 with a p.G2385R variant (11.37%). We failed to detect p.R1441C, p.R1441H, or p.I2020T mutations in this cohort.

The pedigree of the family with the p.R1441G mutation is shown in Fig. 1A. Five members of this family presented with parkinsonism (I:2, I:3, I:6, II:2, and II:5). Direct sequencing analysis of *LRRK2* revealed a heterozygous p.R1441G (*LRRK2* 4321C>G) mutation in II:5 (proband), I:6, and II:2. A healthy brother (II:4) of the proband did not share the mutation (Fig. 1B). Two individuals (II:2: a first cousin of the proband with the p.R1441G mutation, 50-year-old female; and II:4: a healthy brother of the proband without the p.R1441G mutation, 35-year-old male) were heterozygous for the p.G2385R (*LRRK2* 7153G>A) variant, which was observed on a different haplotype to that in individuals with the p.R1441G mutation. These results show co-segregation of parkinsonism and the mutation in the family, although the remaining members were unable to be tested.

Genotypes for 15 markers from our patients (II:2 and II:5) and the corresponding haplotype shared among 29 p.R1441G carriers from Spanish families are presented in Table 1. Allele sharing was evident at only 3 of the 15 markers and was not observed at c.4937T>C (p.M1646T), a rare polymorphism immediately flanking c.4321C>G (p.R1441G). Thus, our Japanese family members do not share a common founder with the Spanish families.

3.2. Case reports

The clinicoradiological findings in these patients are summarized in Table 2.

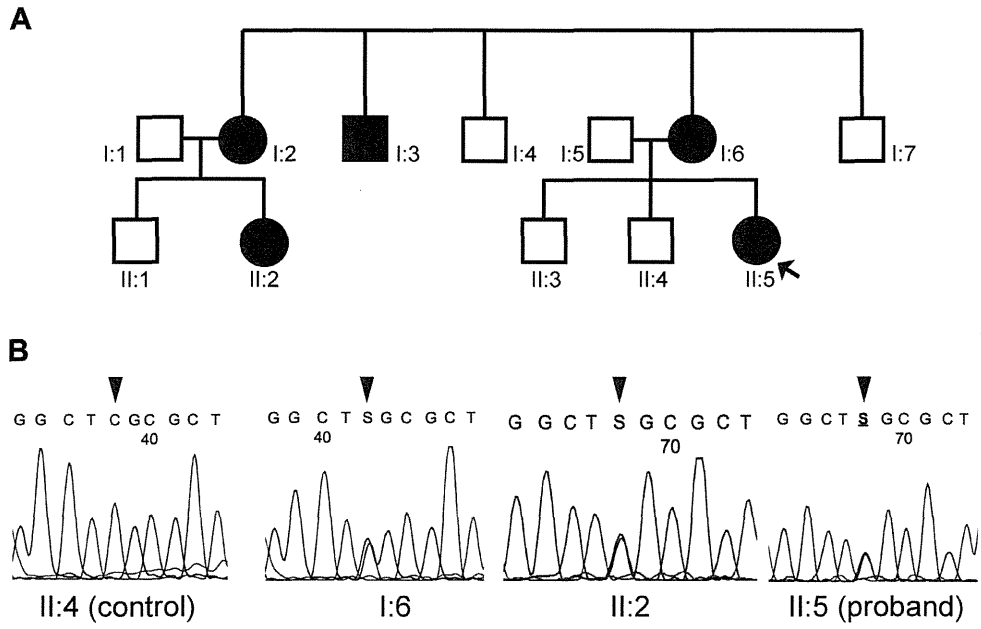

Fig. 1. Pedigree and direct sequencing analysis of the Japanese family with the *LRRK2* p.R1441G mutation. (A) Pedigree of the Japanese family with the *LRRK2* p.R1441G mutation. The arrow indicates the proband. (B) Direct sequencing analysis of *LRRK2* in this family. Arrow heads indicate sites of heterozygous substitution of *LRRK2* 4321C>G.

Table 1
Comparison of R1441G-containing haplotypes across the *LRRK2* region

Location	Marker	Spanish-Basque	Uruguay	II:2	II:5
33305760	D12S2080	**188**	**188**/192	192	192
34142287	rs1511547	**T**	C	C	C
34142413	rs55917927	**C**	T	T	T
34142467	rs56260627	**A**	G	G	G
37708307	rs10876410	**A**	**A**	**A**	**A**
38738007	D12S2194	**249**	253/257	253	253
LRRK2	D12S2516	**252**	254	**252**/254	**252**/254
	R1441 G	**G**	**G**/C	**G**/C	**G**/C
	M1646 T	**C**	T	T	T
	D12S2518	**154**	**154**	**154**	**154**
39116885	D12S2519	**138**	132/140	132/140	132/140
39120098	D12S2520	**248**	257	257	257
39128754	D12S2521	**323**	319/359	315	315
39132380	D12S2522	**281**	283/297	283/297	283/297
39176380	D12S2517	**184**	188/198	202	202
39312730	D12S1048	**211**	**211**/214	220	220

"Spanish-Basque" indicates the haplotype shared among patients with the *LRRK2* p.R1441G mutation from northern Spain. In the members of Japanese family, allele sharing was observed at only 5 markers, indicated in bold.

3.2.1. p.R1441G-Patient II:5

This 36-year-old female developed clumsiness in the right hand and leg at the age of 34 years. Subsequently, she developed right leg tremor and gait disturbance. She did not have any problems with cognition, sleep, or bowel movements. Neurologic examination revealed hemiparkinsonism including resting tremor, muscular rigidity, and akinesia in her right upper and lower limbs along with hyperreflexia in all extremities. Her motor score on the unified PD rating scale (UPDRS part III) was 17 points (Supplementary Video 1). Neurocognitive assessments, such as the Mini Mental State Examination, Frontal Assessment Battery (FAB), and the Japanese version of the Montreal cognitive assessment (MoCA-J) were normal. The odor stick identification test for Japanese revealed mild hyposmia. The administration of levodopa/benserazide (200 mg/50 mg), pramipexole (4 mg), and selegiline (5 mg) resulted in a marked amelioration of her parkinsonism without psychiatric problems. After treatment, her UPDRS part III score was 4 points. Although she did not have any cerebrovascular risk factors, fluid level attenuated inversion recovery (FLAIR) magnetic resonance imaging (MRI) revealed bilateral scattered deep white matter lesions with no structural abnormality (Fig. 2C–F). The results of iodine-123 metaiodobenzylguanidine (^{123}I-MIBG) myocardial scintigraphy were normal (Fig. 2B). Iodine-123 iodoamphetamine single photon emission computed tomography (^{123}I-IMP SPECT) revealed normal regional cerebral blood flow (rCBF) (Fig. 2A).

3.2.2. p.R1441G-Patient I:6

This 65-year-old female is the mother of Patient II:5. Her sister (I:2) and brother (I:3) were also diagnosed as having PD in middle age with no detailed history obtained. She had a history of depression, insomnia over the past 12 years, and right frontoparietal traumatic injury at the age of 55 years. At the age of 60 years, sulpiride (150 mg/d) was administrated for depression, resulting in the development of parkinsonism. Cessation of sulpiride ameliorated her parkinsonism and brotizolam (0.25 mg/d), paroxetine (10 mg/d), zolpidem (5 mg/d), flunitrazepam (2 mg/d), etizolam (1.5 mg/d), and trazodone (50 mg/d) were given for the treatment of her depression and insomnia. At the age of 65 years, she impulsively attempted suicide. The administration of perospirone (12 mg/d) induced a marked deterioration of her motor and swallowing functions. After cessation of perospirone, quetiapine (37.5 mg/d) was used to treat her psychiatric symptoms without aggravation of motor function. Three weeks after the suicide attempt, neurologic examinations revealed minimal left-dominant parkinsonism (Supplementary Video 2) and mild hyposmia (odor stick identification test for Japanese; 6 points).

Although she did not have any problems with orientation, memory, and calculation, the FAB and MoCA-J revealed dysfunctions of verbal fluency and conceptualization (FAB and MoCA-J scores of 14/18 and 24/30, respectively). Although she did not have any cerebrovascular risk factors, T2-weighted, and FLAIR MRI revealed frontotemporal atrophy and small abnormal high intensity lesions in the bilateral frontal white matter (Fig. 2I–L). The results of ^{123}I-MIBG myocardial scintigraphy were normal (Fig. 2H). ^{123}I-IMP SPECT showed decreased rCBF in the bilateral frontal lobes, corresponding to the cranial MRI (Fig. 2G).

3.2.3. p.R1441G-Patient II:2

This 50-year-old female is a first cousin of Patient II:5. She carries both p.R1441G and p.G2385R mutations in *LRRK2*. She had panic syndrome at the age of 18 years. She developed bradykinesia and tremor in the left lower limb at the age of 28 years. On neurologic examination, 2 years after disease onset, she showed left hemiparkinsonism and hyperreflexia in all extremities without any cognitive dysfunction. The administration of levodopa/carbidopa (200 mg/20 mg), trihexyphenidyl (3 mg), talipexole (2.4 mg), and pergolide (0.3 mg) resulted in a marked amelioration of her parkinsonism. Cranial FLAIR MRI was normal and ^{123}I-IMP SPECT showed decreased rCBF in the right basal ganglia (Fig. 2M–O). After the third year of her illness, she developed motor fluctuations with severe ballistic dyskinesia in the left lower limb as a result of high doses of anti-parkinsonian medications. After the 11th year of her illness, bilateral deep brain stimulation of the subthalamic nucleus (STN-DBS) was performed (Fig. 2P). Although STN-DBS was able to temporarily ameliorate her motor complications, she developed dystonic motor complications owing to right-sided STN-DBS stimulation 3 months after the commencement of DBS. In addition, she showed schizophrenic psychosis with severe delusions associated with STN-DBS at 1 year after the operation. After the 13th year of illness, she showed severe wearing off and dyskinesia with off-time pain and dopamine dysregulation syndrome. The left-sided STN-DBS partially ameliorated her off-phase painful dystonia, but caused severe dyskinesia in the on-phase. Eventually, she was put on levodopa/benserazide (700 mg/175 mg/d) and quetiapine (25 mg/d) using left-side STN-DBS in the off-phase only, enabling her to enjoy bowling and ride a bicycle in the on-phase. However, in the off-phase, she showed severe akinesia and panic attacks with delusional ideation.

3.2.4. Other mutations

A 58-year-old male with PD due to p.G2019S, whose father and 2 of 5 siblings had PD developed levodopa-responsive parkinsonism, including resting tremor, rigidity, postural instability, and right lower-limb akinesia without cognition and autonomic dysfunctions. The results of ^{123}I-MIBG myocardial scintigraphy were normal. ^{123}I-IMP SPECT showed decreased rCBF in the frontal lobe, basal ganglia, and bilateral thalamus (Table 2).

Approximately 80% of patients with the p.G2385R variant showed typical parkinsonism with levodopa effectiveness. Autonomic dysfunction is present in <20% of them. In 60% of them, the results of ^{123}I-MIBG myocardial scintigraphy were normal (Table 2).

4. Discussion

Here, we report for the first time an *LRRK2* p.R1441G mutation in Asia. Whereas the p.R1441G mutation is the most prevalent mutation in the Basque country, it is extremely rare outside of northern Spain (Haugarvoll and Wszolek, 2009; Marti-Masso et al.,

Table 2
Clinical features of patients with *LRRK2* p.R1441G mutation

	p.R1441G our cohort			p.G2019S our cohort	p.G2385R our cohort	p.R1441G northern Spain	p.R1441G Uruguay	iPD
	Patient II:5	Patient I:6	Patient II:2					
Age at onset (y)	34	55	28	54	52 (21–83)	55 (29–80)	50	Around 60
Disease duration (y)	2	10	16	4	7		4	
Resting tremor	+	−	+	+	59%	+	+	+
Bradykinesia	+	+	+	+	86.7%	+	+	+
Rigidity	+	+	+	+	82.9%	+	+	+
Gait disturbance	+	−	+	+	80%	+	N.A.	+
Postural instability	−	−	+	+	62.9%	+	+	+
Clinical response to levodopa	+	N.A.	+	+	69.5%	+	+	+
Wearing off	−	−	+	N.A.	28.6%	+	N.A.	+
Levodopa-induced dyskinesia	−	−	+	N.A.	24.8%	+	N.A.	+
Asymmetry at onset	+	+	+	+	73.3%	+	+	+
Hyposmia (OSIT-J)	Mild impairment (9, cutoff; 11.09[a])	Mild impairment (6, cutoff; 9.78[a])	N.A.	N.A.	N.A.	Mild impairment	N.A.	Severe impairment
Orthostatic hypotension	−	−	−	−	12.4%	−	N.A.	+
Incontinence	−	−	−	−	18.1%	−	N.A.	+
Sleep benefit	+	−	Unknown	−	16.2%	−	N.A.	−
Dystonia at onset	−	−	−	N.A.	14.3%	−	N.A.	−
Hyperreflexia	+	−	+	N.A.	17.1%	−	N.A.	−
Hallucination	−	−	+	−	16.2%	−	N.A.	−
Dementia (FAB/MMSE/MoCA-J)	− (18/30/29)	Slt. frontal dysfunction (14/N.A./24)	−	−	12.4%	−	−	−
Other psychiatric problems	−	Depression, executive dysfunction	S-like, delusion	−	±	±	N.A.	−
Brain MRI	Abnormal small spots scatter in white matter	Abnormal small spots scatter in white matter, bilateral frontal lobe atrophy, post traumatic hemorrhage in right frontoparietal cortex	No abnormality	N.A.	N.A.	No abnormality	N.A.	No abnormality
^{123}I-IMP SPECT	Normal record	Decreased rCBF in bil. frontal lobes	Decreased rCBF in the right basal ganglia	Decreased rCBF in frontal, basal ganglia, and right thalamus	N.A.	N.A.	N.A.	Decreased rCBF in bil. occipital lobes
^{123}I-MIBG myocardiac scintigraphy	H/M ratio (E/L) = 2.38/2.68; cutoff, 1.4[b]; wash out ratio= 4.15%	H/M ratio (E/L) = 3.18/3.63; cutoff, 2.0[b]; wash out ratio = 20.1%	Not performed	Normal	Decreased 40%, normal 60%	Less decreased than PD	N.A.	Decreased H/M ratio

Key: Bil., bilateral; H/M, heart/mediastinum ratio; FAB, frontal assessment battery; ^{123}I-MIBG, iodine-123 metaiodobenzylguanidine; iPD, idiopathic Parkinson's disease; MMSE, mini mental state examination; MoCA-J, Japanese version of the Montreal cognitive assessment; MRI, magnetic resonance imaging; N.A., not applicable; OSIT-J, odor stick identification test for Japanese; PD, Parkinson's disease; rCBF, regional cerebral blood flow; S-like, schizophrenic-like; Slt., slightly.

[a] Cutoff points in OSIT-J vary according to age and sex.

[b] Cutoff points in ^{123}I-MIBG myocardiac scintigraphy were different in every institution.

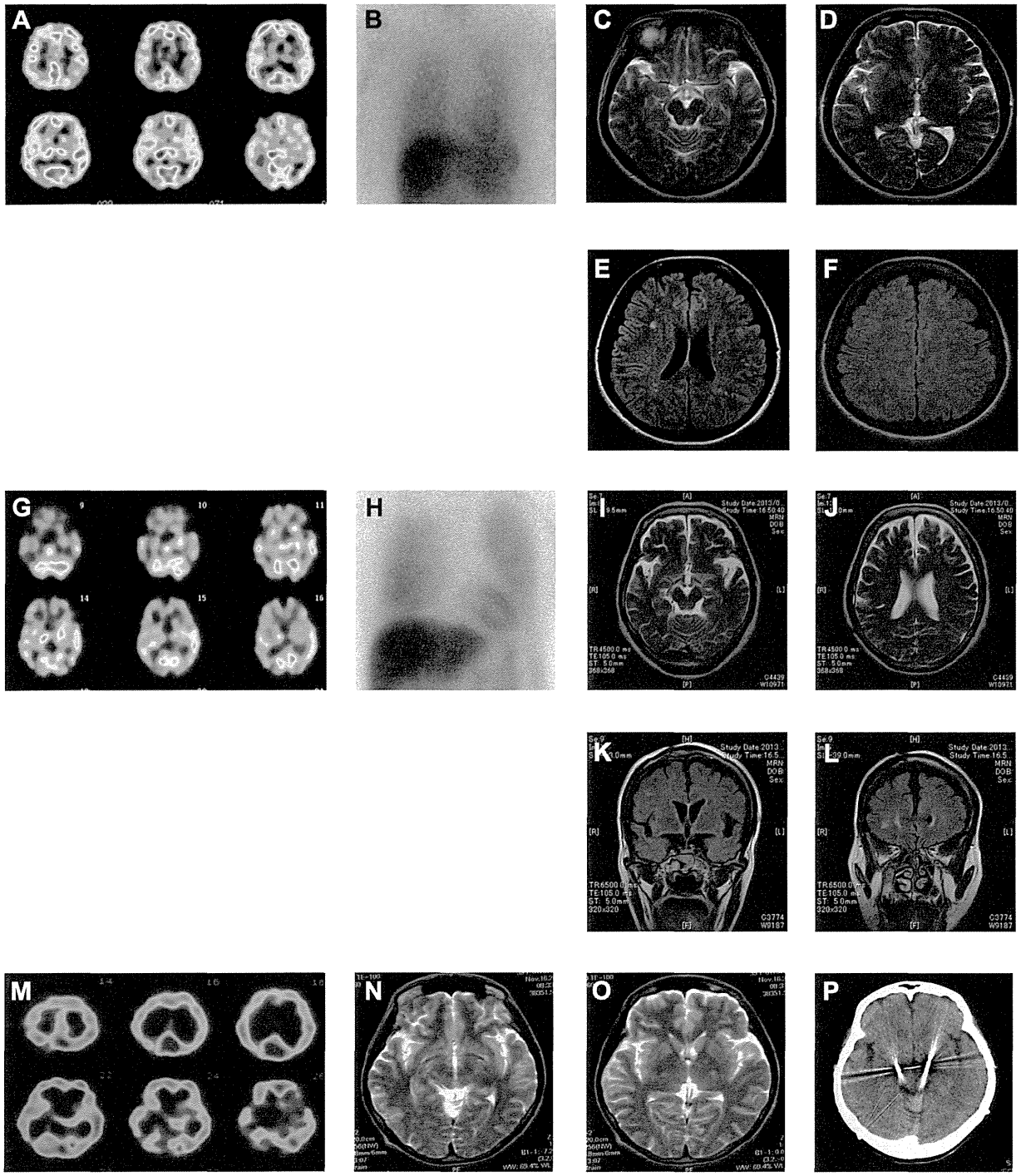

Fig. 2. Cranial MRI, CT, ^{123}I-IMP SPECT, and ^{123}I-MIBG myocardial scintigraphy of Patients II:5, I:6, and II:2. In Patient II:5, ^{123}I-IMP SPECT and ^{123}I-MIBG myocardial scintigraphy show no abnormality (A, B). Cranial T2-WI and FLAIR MRI depict several abnormal high-intensity lesions without any atrophy (C–F). In Patient I:6, ^{123}I-IMP SPECT shows hypoperfusion of bilateral frontal area (G). Cranial T2-WI and FLAIR MRI show several abnormal high-intensity lesions with frontal lobe atrophy (I–L). The results of ^{123}I-MIBG myocardial scintigraphy were normal (E). In Patient II:2, ^{123}I-IMP SPECT shows hypoperfusion of the right basal ganglia (M). Cranial T2-WI MRI showing no abnormality (O, P). Cranial CT showed that electrodes for deep brain stimulation of the subthalamic nucleus were implanted into the bilateral subthalamic nucleus (N). Abbreviations: CT, computerized tomography; FLAIR, fluid level attenuated inversion recovery; ^{123}I-IMP SPECT, Iodine-123 iodoamphetamine single photon emission computed tomography; ^{123}I-MIBG, iodine-123 metaiodobenzylguanidine; MRI, magnetic resonance imaging.

2009; Mata et al., 2005, 2009b; Simon-Sanchez et al., 2006). In our family, the lack of sharing at p.M1646T (Table 1), located 9.7 kb downstream from the mutation, is particularly informative because the "*LRRK2* c.4937 T>C" allele occurs at a frequency of <2% in controls from northern Spain but has been observed in all mutation carriers described in the literature (Mata et al., 2005). Therefore, we concluded that our family has a different haplotype from that of all the Spanish families reported to date. Recently, a cohort study revealed a Uruguayan patient carrying a p.R1441G mutation, who did not share the haplotype of the original Spanish

families (Mata et al., 2009a). Our patients did not appear to have an ancestor from outside Japan based on historical records. Thus, they are only the second family with this mutation outside of Spain, with a different haplotype, reinforcing the hypothesis that p.R1441 is a mutational hot spot. It is therefore possible that patients with a mutation at *LRRK2* p.R1441 are distributed worldwide.

Previous reports have described that the clinical features of the original Basque family members (Paisan-Ruiz et al., 2005) and the Uruguayan patient (Mata et al., 2009a) with *LRRK2* p.R1441G were similar to those of typical idiopathic PD (iPD), including good response to levodopa therapy, rigidity, and akinesia (Table 2). Although most of the members of the Basque families showed late-onset PD (Gonzalez-Fernandez et al., 2007; Mata et al., 2005; Simon-Sanchez et al., 2006), Gonzalez-Fernandez et al. (2007) reported that 5 of 15 patients showed an early age at onset (<50 years). These findings indicate that some of the Basque families might exhibit intrafamilial clinical heterogeneity. In our Japanese family, Patients II:2 and II:5 also showed younger age at onset compared with iPD patients. In contrast to Patients I:2, I:3, II:2, and II:5, Patient I:6, albeit in old age, showed trivial hemiparkinsonism only detected by detailed neurologic examination with no functional disabilities, whereas the patient showed frontal dysfunction with impaired verbal fluency and conceptualization. Severe psychosis appeared to be unique to Patient II:2 in our family. Therefore, our family also exhibited intrafamilial clinical heterogeneity. The presence of such heterogeneity suggests that additional factors, that is, genetic and/or environmental factors, contribute to the development of the disease in association with the p.R1441G mutation.

Based on the results of 2 studies, patients with the *LRRK2* p.R1441G mutation seem to display fewer of the non-motor features characteristic of iPD, such as hyposmia and cardiac sympathetic denervation (Table 2) (Ruiz-Martinez et al., 2011; Tijero et al., 2013). Consistent with these observations, our patients showed no autonomic dysfunctions, including bowel and urinary dysfunctions and orthostatic hypotension, REM-sleep behavior disorders, or reduced cardiac ^{123}I-MIBG uptake (Table 2). Hyposmia detected in our patients (II:5 and I:6) appeared less severe than that in iPD, requiring further studies to determine whether the p.R1441G mutation is associated with hyposmia. In terms of neuroimaging, we also observed differences between patients with the p.R1441G mutation and iPD patients. Patient I:6 showed frontal atrophy on MRI and frontal hypoperfusion on ^{123}I-IMP SPECT. Furthermore, ^{123}I-IMP SPECT of Patient II:2 revealed hypoperfusion in the basal ganglia. These findings contrast with those in iPD patients, which typically show a decrement of blood flow in the occipital lobes (Abe et al., 2003). On the basis of these results, the phenotypes of our patients seemed to be different from those of iPD patients with Lewy pathology. Pathologic findings in PD patients with *LRRK2* mutations are very variable despite them exhibiting a relatively uniform clinical phenotype of parkinsonism (Cookson et al., 2008; Hasegawa et al., 2009; Ross et al., 2006; Ujiie et al., 2012; Zimplich et al., 2004). A clinicopathological study of patients with the p.G2019S mutation revealed no correlation between Lewy pathology and clinical phenotypes, including dementia and psychiatric symptoms (Ross et al., 2006). These observations suggest that additional factors besides LRRK2 mutations could play roles in the development of dementia and/or psychiatric problems as well as Lewy pathology. It therefore remains to be clarified whether our cases show Lewy pathology, although a previously reported patient with a p.R1441G mutation did not have Lewy pathology (Marti-Masso et al., 2009).

It has been described that the phenotype of PD patients with the p.G2019S mutation cannot be distinguished from iPD (Haugarvoll and Wszolek, 2009). However, the patient with the p.G2019S mutation in our cohort showed no autonomic dysfunction, no psychosis, no dementia, and normal cardiac ^{123}I-MIBG uptake, resembling the phenotype of p.R1441G-patient II:5 without early age of onset. The prevalence of autonomic dysfunctions of PD patients with p.G2385R was also seemed to be less than that in iPD patients (Khoo et al., 2013). Two members (II:2 and II:4) of our family also had the p.G2385R variant. Although combining p.R1441G with p.G2385R in II:2 might cause severe psychosis, it remains unclear whether the p.G2385R variant combined with an LRRK2 pathogenic mutation might be associated with a deterioration of clinical phenotypes. Therefore, we could not determine the contribution of this variant to the phenotypic modifications in our family.

In Patient II:2, STN-DBS exacerbated psychiatric problems without any improvement of motor function. Gomez-Esteban et al. (2008) also described a poor response to STN-DBS therapy in patients with the p.R1441G mutation. These results might be attributable to the p.R1441G mutation.

We found 1 patient with the p.G2019S mutation (0.11%) in this cohort. Parkinsonism because of p.G2019S is common in Caucasian populations (Haugarvoll and Wszolek, 2009), and the frequencies in the Ashkenazi Jewish and North African Arab cohorts are 18.3% and 39%, respectively (Lesage et al., 2006; Ozelius et al., 2006). However, this mutation has been reported to be very rare in Asian populations (Tan et al., 2005; Tomiyama et al., 2006; Zabetian et al., 2006), consistent with our cohort. The finding of a relatively high prevalence of the *LRRK2* p.G2385R variant in our cohort is consistent with the findings of previous reports (Funayama et al., 2007; Ross et al., 2011). Although Ross et al. (2011) described that the prevalence of PD with p.G2385R in large Asian populations, including Japanese was about 3%, the prevalence of p.G2385R in the previously reported Japanese cohort was 11.6% (Funayama et al., 2007), similar to that in the present cohort. On the other hand, the association of p.G2385R with PD in the Caucasian population was not supported by the results of a previous large population study (Ross et al., 2011).

To the best of our knowledge, this is the first report of an *LRRK2* p.R1441G mutation in Asia and only the third outside of northern Spain (Mata et al., 2009a). Further mutation screening of *LRRK2* p.R1441G in Asian populations may confirm the characteristic features of patients with this mutation.

Disclosure statement

The authors report no conflicts of interest and have no financial interest related to the material described in the manuscript.

Acknowledgements

The authors thank Dr Hideo Mori (Juntendo Koshigaya Hospital) and all the participants in this study. This work was supported by a Strategic Research Foundation Grant-in-Aid Project for Private Universities, Grants-in-Aid for Scientific Research (KAKENHI) (to Nobutaka Hattori, 24390224 and to Taku Hatano, 25461290) and a Grant-in-Aid for Scientific Research on Innovative Areas (to Nobutaka Hattori, 23111003 and to Manabu Funayama, 25129707) from the Japanese Ministry of Education, Culture, Sports, Science and Technology. This work was also supported by grants from the Parkinson's Disease Foundation, United States and the National Institutes of Health, United States (R01 NS065070 and P50 NS062684).Appendix A. Supplementary dataSupplementary Video 1. Supplementary Video 2.

Appendix A. Supplementary data

Supplementary data associated with this article can be found, in the online version, at http://dx.doi.org/10.1016/j.neurobiolaging.2014.05.025.

References

Abe, Y., Kachi, T., Kato, T., Arahata, Y., Yamada, T., Washimi, Y., Iwai, K., Ito, K., Yanagisawa, N., Sobue, G., 2003. Occipital hypoperfusion in Parkinson's disease without dementia: correlation to impaired cortical visual processing. J. Neurol. Neurosurg. Psychiatry 74, 419–422.

Cookson, M.R., Hardy, J., Lewis, P.A., 2008. Genetic neuropathology of Parkinson's disease. Int. J. Clin. Exp. Pathol. 1, 217–231.

Cornejo-Olivas, M.R., Torres, L., Mazzetti, P., Cosentino, C., Zabetian, C.P., Mata, I.F., 2013. Variable penetrance of the LRRK2-R1441G mutation in a Peruvian family [abstract]. Mov. Disord. 23 (Suppl. 1), 1154.

Deng, H., Le, W., Guo, Y., Hunter, C.B., Xie, W., Huang, M., Jankovic, J., 2006. Genetic analysis of LRRK2 mutations in patients with Parkinson disease. J. Neurol. Sci. 251, 102–106.

Funayama, M., Li, Y., Tomiyama, H., Yoshino, H., Imamichi, Y., Yamamoto, M., Murata, M., Toda, T., Mizuno, Y., Hattori, N., 2007. Leucine-rich repeat kinase 2 G2385R variant is a risk factor for Parkinson disease in Asian population. Neuroreport 18, 273–275.

Gomez-Esteban, J.C., Lezcano, E., Zarranz, J.J., Gonzalez, C., Bilbao, G., Lambarri, I., Rodriguez, O., Garibi, J., 2008. Outcome of bilateral deep brain subthalamic stimulation in patients carrying the R1441G mutation in the LRRK2 dardarin gene. Neurosurgery 62, 857–863.

Gonzalez-Fernandez, M.C., Lezcano, E., Ross, O.A., Gomez-Esteban, J.C., Gomez-Busto, F., Velasco, F., Alvarez-Alvarez, M., Rodriguez-Martinez, M.B., Ciordia, R., Zarranz, J.J., Farrer, M.J., Mata, I.F., de Pancorbo, M.M., 2007. Lrrk2-associated parkinsonism is a major cause of disease in Northern Spain. Parkinsonism Relat. Disord. 13, 509–515.

Hasegawa, K., Stoessl, T., Yokoyama, T., Kowa, H., Wszolek, Z.K., Yagishita, S., 2009. Familial parkinsonism: study of original Sagamihara PARK8 (I2020T) kindred with variable clinicopathologic outcomes. Parkinsonism Relat. Disord. 15, 300–306.

Haugarvoll, K., Wszolek, Z.K., 2009. Clinical features of LRRK2 parkinsonism. Parkinsonism Relat. Disord. 15 (Suppl. 3), S205–S208.

Haugarvoll, K., Rademakers, R., Kachergus, J.M., Nuytemans, K., Ross, O.A., Gibson, J.M., Tan, E.K., Gaig, C., Tolosa, E., Goldwurm, S., Guidi, M., Riboldazzi, G., Brown, L., Walter, U., Benecke, R., Berg, D., Gasser, T., Theuns, J., Pals, P., Cras, P., De Deyn, P.P., Engelborghs, S., Pickut, B., Uitti, R.J., Foroud, T., Nichols, W.C., Hagenah, J., Klein, C., Samii, A., Zabetian, C.P., Bonifati, V., Van Broeckhoven, C., Farrer, M.J., Wzolek, Z.K., 2008. Lrrk2 R1441C parkinsonism is clinically similar to sporadic Parkinson disease. Neurology 70, 1456–1460.

Khoo, T.K., Yarnall, A.J., Duncan, G.W., Coleman, S., O'Brien, J.T., Brooks, D.J., Barker, R.A., Burn, D.J., 2013. The spectrum of nonmotor symptoms in early Parkinson disease. Neurology 80, 276–281.

Lesage, S., Durr, A., Tazir, M., Lohmann, E., Leutenegger, A.L., Janin, S., Pollak, P., Brice, A., French Parkinson's Disease Genetics Study Group, 2006. LRRK2 G2019S as a cause of Parkinson's disease in North African Arabs. N. Engl. J. Med. 354, 422–423.

Marti-Masso, J.F., Ruiz-Martinez, J., Bolano, M.J., Ruiz, I., Gorostidi, A., Moreno, F., Ferrer, I., Lopez de Munain, A., 2009. Neuropathology of Parkinson's disease with the R1441G mutation in LRRK2. Mov. Disord. 24, 1998–2001.

Mata, I.F., Taylor, J.P., Kachergus, J., Hulihan, M., Huerta, C., Lahoz, C., Blazquez, M., Guisasola, L.M., Salvador, C., Ribacoba, R., Martinez, C., Farrer, M., Alvarez, V., 2005. LRRK2 R1441G in Spanish patients with Parkinson's disease. Neurosci. Lett. 382, 309–311.

Mata, I.F., Cosentino, C., Marca, V., Torres, L., Mazzetti, P., Ortega, O., Raggio, V., Aljanati, R., Buzo, R., Yearout, D., Dieguez, E., Zabetian, C.P., 2009a. LRRK2 mutations in patients with Parkinson's disease from Peru and Uruguay. Parkinsonism Relat. Disord. 2009, 370–373.

Mata, I.F., Hutter, C.M., Gonzalez-Fernandez, M.C., de Pancorbo, M.M., Lezcano, E., Huerta, C., Blazquez, M., Ribacoba, R., Guisasola, L.M., Salvador, C., Gomez-Esteban, J.C., Zarranz, J.J., Infante, J., Jankovic, J., Deng, H., Edwards, K.L., Alvarez, V., Zabetian, C.P., 2009b. Lrrk2 R1441G-related Parkinson's disease: evidence of a common founding event in the seventh century in Northern Spain. Neurogenetics 10, 347–353.

Ozelius, L.J., Senthil, G., Saunders-Pullman, R., Ohmann, E., Deligtisch, A., Tagliati, M., Hunt, A.L., Klein, C., Henick, B., Hailpern, S.M., Lipton, R.B., Soto-Valencia, J., Risch, N., Bressman, S.B., 2006. LRRK2 G2019S as a cause of Parkinson's disease in Ashkenazi Jews. N. Engl. J. Med. 354, 424–425.

Paisan-Ruiz, C., Jain, S., Evans, E.W., Gilks, W.P., Simon, J., van der Brug, M., Lopez de Munain, A., Aparicio, S., Gil, A.M., Khan, N., Johnson, J., Martinez, J.R., Nicholl, D., Carrera, I.M., Pena, A.S., de Silva, R., Lees, A., Marti-Masso, J.F., Perez-Tur, J., Wood, N.W., Singleton, A.B., 2004. Cloning of the gene containing mutations that cause PARK8-linked Parkinson's disease. Neuron 44, 595–600.

Paisan-Ruiz, C., Saenz, A., Lopez de Munain, A., Marti, I., Martinez Gil, A., Marti-Masso, J.F., Perez-Tur, J., 2005. Familial Parkinson's disease: clinical and genetic analysis of four Basque families. Ann. Neurol. 57, 365–372.

Ross, O.A., Toft, M., Whittle, A.J., Johnson, J.L., Papapetropoulos, S., Mash, D.C., Litvan, I., Gordon, M.F., Wszolek, Z.K., Farrer, M.J., Dickson, D.W., 2006. Lrrk2 and Lewy body disease. Ann. Neurol. 59, 388–393.

Ross, O.A., Spanaki, C., Griffith, A., Lin, C.H., Kachergus, J., Haugarvoll, K., Latsoudis, H., Plaitakis, A., Ferreira, J.J., Sampaio, C., Bonifati, V., Wu, R.M., Zabetian, C.P., Farrer, M.J., 2009. Haplotype analysis of Lrrk2 R1441H carriers with parkinsonism. Parkinsonism Relat. Disord. 15, 466–467.

Ross, O.A., Soto-Ortolaza, A.I., Heckman, M.G., Aasly, J.O., Abahuni, N., Annesi, G., Bacon, J.A., Bardien, S., Bozi, M., Brice, A., Brighina, L., Van Broeckhoven, C., Carr, J., Chartier-Harlin, M.C., Dardiotis, E., Dickson, D.W., Diehl, N.N., Elbaz, A., Ferrarese, C., Ferraris, A., Fiske, B., Gibson, J.M., Gibson, R., Hadjigeorgiou, G.M., Hattori, N., Ioannidis, J.P., Jasinska-Myga, B., Jeon, B.S., Kim, Y.J., Klein, C., Kruger, R., Kyratzi, E., Lesage, S., Lin, C.H., Lynch, T., Maraganore, D.M., Mellick, G.D., Mutez, E., Nilsson, C., Opala, G., Park, S.S., Puschmann, A., Quattrone, A., Sharma, M., Silburn, P.A., Sohn, Y.H., Stefanis, L., Tadic, V., Theuns, J., Tomiyama, H., Uitti, R.J., Valente, E.M., van de Loo, S., Vassilatis, D.K., Vilarino-Guell, C., White, L.R., Wirdefeldt, K., Wszolek, Z.K., Wu, R.M., Farrer, M.J., Genetic Epidemiology Of Parkinson's Disease, Consortium, 2011. Association of LRRK2 exonic variants with susceptibility to Parkinson's disease: a case–control study. Lancet Neurol. 10, 898–908.

Ruiz-Martinez, J., Gorostidi, A., Goyenechea, E., Alzualde, A., Poza, J.J., Rodriguez, F., Bergareche, A., Moreno, F., Lopez de Munain, A., Marti Masso, J.F., 2011. Olfactory deficits and cardiac 123I-MIBG in Parkinson's disease related to the LRRK2 R1441G and G2019S mutations. Mov. Disord. 26, 2026–2031.

Simon-Sanchez, J., Marti-Masso, J.F., Sanchez-Mut, J.V., Paisan-Ruiz, C., Martinez-Gil, A., Ruiz-Martinez, J., Saenz, A., Singleton, A.B., Lopez de Munain, A., Perez-Tur, J., 2006. Parkinson's disease due to the R1441G mutation in Dardarin: a founder effect in the Basques. Mov. Disord. 21, 1954–1959.

Tan, E.K., Shen, H., Tan, L.C., Farrer, M., Yew, K., Chua, E., Jamora, R.D., Puvan, K., Puong, K.Y., Zhao, Y., Pavanni, R., Wong, M.C., Yih, Y., Skipper, L., Liu, J.J., 2005. The G2019S LRRK2 mutation is uncommon in an Asian cohort of Parkinson's disease patients. Neurosci. Lett. 384, 327–329.

Tijero, B., Gomez Esteban, J.C., Somme, J., Llorens, V., Lezcano, E., Martinez, A., Rodriguez, T., Berganzo, K., Zarranz, J.J., 2013. Autonomic dysfunction in parkinsonian LRRK2 mutation carriers. Parkinsonism Relat. Disord. 19, 906–909.

Tomiyama, H., Li, Y., Funayama, M., Hasegawa, K., Yoshino, H., Kubo, S.I., Sato, K., Hattori, T., Lu, C.S., Inzelberg, R., Djaldetti, R., Melamed, E., Amouri, R., Gouider-Khouja, N., Hentati, F., Hatano, Y., Wang, M., Imamichi, Y., Mizoguchi, K., Miyajima, H., Obata, F., Toda, T., Farrer, M.J., Mizuno, Y., Hattori, N., 2006. Clinicogenetic study of mutations in LRRK2 exon 41 in Parkinson's disease patients from 18 countries. Mov. Disord. 21, 1102–1108.

Ujiie, S., Hatano, T., Kubo, S.I., Imai, S., Sato, S., Uchihara, T., Yagishita, S., Hasegawa, K., Kowa, H., Sakai, F., Hattori, N., 2012. LRRK2 I2020T mutation is associated with tau pathology. Parkinsonism Relat. Disord. 18, 819–823.

Yescas, P., Lopez, M., Monroy, N., Boll, M.C., Rodriguez-Violante, M., Rodriguez, U., Ochoa, A., Alonso, M.E., 2010. Low frequency of common LRRK2 mutations in Mexican patients with Parkinson's disease. Neurosci. Lett. 485, 79–82.

Zabetian, C.P., Morino, H., Ujike, H., Yamamoto, M., Oda, M., Maruyama, H., Izumi, Y., Kaji, R., Griffith, A., Leis, B.C., Roberts, J.W., Yearout, D., Samii, A., Kawakami, H., 2006. Identification and haplotype analysis of LRRK2 G2019S in Japanese patients with Parkinson disease. Neurology 67, 697–699.

Zimprich, A., Biskup, S., Leitner, P., Lichtner, P., Farrer, M., Lincoln, S., Kachergus, J., Hulihan, M., Uitti, R.J., Calne, D.B., Stoessl, A.J., Pfeiffer, R.F., Patenge, N., Carbajal, I.C., Vieregge, P., Asmus, F., Muller-Myhsok, B., Dickson, D.W., Meitinger, T., Strom, T.M., Wszolek, Z.K., Gasser, T., 2004. Mutations in LRRK2 cause autosomal-dominant parkinsonism with pleomorphic pathology. Neuron 44, 601–607.

Neuroradiology (2014) 56:251–258
DOI 10.1007/s00234-014-1327-1

FUNCTIONAL NEURORADIOLOGY

A preliminary diffusional kurtosis imaging study of Parkinson disease: comparison with conventional diffusion tensor imaging

Koji Kamagata · Hiroyuki Tomiyama · Taku Hatano · Yumiko Motoi · Osamu Abe · Keigo Shimoji · Kouhei Kamiya · Michimasa Suzuki · Masaaki Hori · Mariko Yoshida · Nobutaka Hattori · Shigeki Aoki

Received: 2 December 2013 / Accepted: 15 January 2014 / Published online: 28 January 2014

Abstract
Introduction Diffusional kurtosis imaging (DKI) is a more sensitive technique than conventional diffusion tensor imaging (DTI) for assessing tissue microstructure. In particular, it quantifies the microstructural integrity of white matter, even in the presence of crossing fibers. The aim of this preliminary study was to compare how DKI and DTI show white matter alterations in Parkinson disease (PD).
Methods DKI scans were obtained with a 3-T magnetic resonance imager from 12 patients with PD and 10 healthy controls matched by age and sex. Tract-based spatial statistics were used to compare the mean kurtosis (MK), mean diffusivity (MD), and fractional anisotropy (FA) maps of the PD patient group and the control group. In addition, a region-of-interest analysis was performed for the area of the posterior corona radiata and superior longitudinal fasciculus (SLF) fiber crossing.
Results FA values in the frontal white matter were significantly lower in PD patients than in healthy controls. Reductions in MK occurred more extensively throughout the brain: in addition to frontal white matter, MK was lower in the parietal, occipital, and right temporal white matter. The MK value of the area of the posterior corona radiata and SLF fiber crossing was also lower in the PD group.
Conclusion DKI detects changes in the cerebral white matter of PD patients more sensitively than conventional DTI. In addition, DKI is useful for evaluating crossing fibers. By providing a sensitive index of brain pathology in PD, DKI may enable improved monitoring of disease progression.

Keywords Diffusional kurtosis imaging · Diffusion tensor imaging · Parkinson disease · Tract-based spatial statistics

K. Kamagata (✉) · K. Kamiya · M. Suzuki · M. Hori · M. Yoshida · S. Aoki
Department of Radiology, Juntendo University School of Medicine, 2-1-1 Hongo, Bunkyo-ku, Tokyo 113-8421, Japan
e-mail: kkamagat@juntendo.ac.jp

H. Tomiyama · T. Hatano · Y. Motoi · N. Hattori
Department of Neurology, Juntendo University School of Medicine, Tokyo, Japan

O. Abe
Department of Radiology, Nihon University School of Medicine, Tokyo, Japan

K. Shimoji
Department of Radiology, National Center of Neurology and Psychiatry Hospital, Tokyo, Japan

Abbreviations

DTI	Diffusion tensor imaging
DKI	Diffusional kurtosis imaging
FA	Fractional anisotropy
MD	Mean diffusivity
MK	Mean kurtosis
PD	Parkinson disease
ROI	Region of interest
SLF	Superior longitudinal fasciculus
TBSS	Tract-based spatial statistics

Introduction

Parkinson disease (PD) is a chronic, progressive, and degenerative neurological disorder defined by its motor symptoms (akinesia, resting tremor, and rigidity) and numerous nonmotor symptoms (such as cognitive impairment, depression, and olfactory dysfunction) [1]. In PD, these motor and nonmotor symptoms reflect the widespread progression of underlying pathologies, which include α-synuclein-immunoreactive inclusions in the cytoplasm of neurons

(Lewy bodies) and within neuronal processes (Lewy neurites), loss of dopaminergic projections from the substantia nigra to the striatum, and progressive loss of cholinergic and monoaminergic cortical projections from the nucleus basalis of Meynert [2–6].

Conventional magnetic resonance imaging (MRI) has been unsuccessful for discerning these pathophysiologic changes in PD; because the results are usually nonspecific, the role of MRI is confined to excluding secondary causes of parkinsonism such as vascular lesions. By contrast, diffusion tensor imaging (DTI) in PD provides quantitative measures of microstructural integrity and organization in vivo and is thus more suitable for detecting subtle alterations not evident with conventional MRI [7–12]. Diffusional abnormalities of frontal white matter have been consistently observed in DTI studies of PD patients [9, 13–16]. DTI with region-of-interest (ROI) analyses has revealed changes in fractional anisotropy (FA) in the frontal lobes of PD patients relative to controls [13]. Karagulle et al. used voxel-based analysis in conjunction with DTI to compare PD patients to controls and observed decreased FA bilaterally in the frontal lobes, including the supplementary and presupplementary motor areas [9]. Similarly, Zhan et al. found reduced FA in the frontal lobes, including the precentral gyrus and supplementary motor areas [14].

In traditional DTI theory, a perfect Gaussian distribution is assumed for the movement of water molecules [17]. However, water in biological structures often shows non-Gaussian diffusion because it is restricted by diffusion barriers such as cell membranes and organelles. Therefore, the assumption of Gaussian water diffusion may be inappropriate in biological structures. Diffusional kurtosis imaging (DKI) has been proposed as a natural extension of DTI that enables the quantification of non-Gaussian diffusion [18–21]. In addition to conventional DTI metrics such as mean diffusivity (MD) and FA, an additional metric related to non-Gaussian water diffusion called mean kurtosis (MK) is obtained in DKI, whereby a higher MK value suggests a more hindered and restricted diffusion environment [22]. In contrast to conventional DTI metrics, MK is not limited to anisotropic environments; hence, it especially permits quantification of the microstructural integrity of white matter, even in the presence of crossing fibers.

These properties of MK have led to its application to the brains of patients with PD. Wang et al. reported increased MK in the basal ganglia and substantia nigra using ROI analysis [23]. They found that MK in the ipsilateral substantia nigra showed the best diagnostic performance relative to the conventional diffusion tensor parameter. We also found that FA and MK were reduced in the cingulate fiber tracts in PD patients relative to controls and that MK in the anterior cingulum showed the best diagnostic performance [24]. However, whole-brain voxel-based DKI analyses have yet to be performed in PD patients. Voxel-based analysis is a technique that can identify the changes of diffusion tensor parameter in any part of the whole brain without a prior hypothesis, unlike ROI analysis.

Here, we expanded on our previous work and conducted whole-brain DKI analyses of PD patients and controls by using tract-based spatial statistics (TBSS) [25] implemented in the FMRIB Software Library 4.1.5 (FSL, Oxford Centre for Functional MRI of the Brain, UK; www.fmrib.ox.ac.uk/fsl) and we compared the data with those obtained with conventional DTI parameters. Thus, the aims of this preliminary study were to investigate how white matter is altered in PD as measured with DKI and to compare the results to those previously demonstrated with DTI.

Materials and methods

Subjects

The participants were PD patients who had been diagnosed by neurologists specializing in movement disorders. Each participant fulfilled the UK Parkinson's Disease Society Brain Bank criteria and was found to be at stage I, II, or III on the Hoehn and Yahr scale. All PD patients were taking levodopa and a dopamine decarboxylase inhibitor (benserazide or carbidopa) at the time of the MR imaging and clinical examination. Eighteen months or more after scanning, all patients remained free of atypical parkinsonism and continued to respond satisfactorily to antiparkinsonian therapy. Ten age- and gender-matched control subjects were voluntarily recruited. None of the control subjects had any history of neurologic or psychiatric disorders or showed any abnormal signal in structural MR imaging.

This study was approved by the ethical committee of Juntendo Hospital, Juntendo University, and informed consent was obtained from all the participants before evaluation. The demographic characteristics of the participants are shown in Table 1.

MR imaging

All MR images were obtained by using a 3.0-T system (Achieva; Philips Healthcare, Best, the Netherlands) equipped with an eight-channel head coil for sensitivity-encoding parallel imaging. Regular structural images such as T1-weighted spin-echo images, T2-weighted turbo spin-echo images, and fluid-attenuated inversion recovery images were obtained before acquiring diffusion tensor and kurtosis images.

DKI data were acquired with a spin-echo EPI sequence along 20 isotropic diffusion gradient directions. For each direction, DKI images were acquired with three values of b (0, 1,000, and 2,000 s/mm^2). The sequence parameters were as follows: image orientation, axial; repetition time (TR), 7,041 ms; echo time (TE), 70 ms; diffusion gradient pulse

Table 1 Demographic characteristics of subjects

	Normal controls (n=10)	PD patients (n=12)	P value
Sex, male/female	5:5	6:6	0.42
Age in years, mean (SD)	67.6 (10.1)	65.4 (10.0)	0.82
Disease duration in years, mean (SD)	NA	7.1 (4.5)	NA
Hoehn–Yahr stage (SD)	0	2.6 (0.8)	NA
Levodopa dosage, mg/day, median (SD)	0	322.7 (194.1)	NA

PD Parkinson disease, *SD* standard deviation, *NA* not applicable

duration (δ), 13.3 ms; diffusion gradient separation (Δ), 45.3 ms; number of excitations (NEX), 1; field of view, 240 mm; matrix, 80×80; slice thickness, 3 mm; number of slices, 50; and imaging time, 6 min 26 s.

Diffusion tensor and kurtosis analyses were performed on an independent Windows PC by using the free software dTV II FZRx and Volume-One 1.81 (http://www.volume-one.org), developed by Masutani et al. (The University of Tokyo; diffusion tensor visualizer available at http://www.ut-radiology.umin.jp/people/masutani/dTV.htm) [7, 26, 27]. First, FA and MD maps based on the conventional mono-exponential model were calculated. Because the kurtosis data was generated using multiple values of b, the FA and MD could be calculated by using part of the diffusion kurtosis data. Next, mean DK maps were obtained (Fig. 1). The details of the procedure for calculating the maps were as previously described [19, 22, 28]. As described in previous papers [19, 22], the DK value for a single direction is determined by acquiring data at three or more b values (including b=0) and fitting them to Eq. (1):

$$\ln[S(b)] = \ln[S(0)] - b \times \mathrm{Dapp} + 1/6 \times b2 \times \mathrm{D2app} \times \mathrm{Kapp} \quad (1)$$

where Dapp is the MD for the given direction and Kapp is the apparent kurtosis coefficient, which is dimensionless.

DTI/DKI image processing with TBSS

Voxel-based analysis of the DTI/DKI data was performed with TBSS [21] implemented in FMRIB Software Library 4.1.5 (FSL, Oxford Centre for Functional MRI of the Brain, UK; www.fmrib.ox.ac.uk/fsl). We corrected for distortions due to eddy currents by affine intrasubject registration to the respective individual $b0$ image by means of the EDDYCORRECT procedure implemented in FSL [29]. FA and MD maps for all subjects were calculated by fitting a tensor model to each voxel of the raw diffusion data, using the tool DTIFIT. Nonbrain structures were eliminated by using the brain extraction tool. FA maps of all subjects were aligned to standard Montreal Neurological Institute (MNI152) space by using the nonlinear registration tool FNIRT. Next, the mean FA image was generated and thinned to create the mean FA skeleton, which represented the centers of all tracts common to the groups. The mean FA skeleton was thresholded to FA >0.20 to include the major white matter pathways but exclude peripheral tracts and gray matter. The aligned FA map of each participant was then projected onto this skeleton by assigning to each point on the skeleton the maximum FA in a plane perpendicular to the local skeleton structure. The resulting skeletons were fed into voxel-wise statistics. By applying the original nonlinear registration of the FA of each subject to the standard space, the MD map was also projected onto the mean FA skeleton. The MD data were used to calculate voxel-wise statistics as well. Voxel-wise statistics of the skeletonized FA data were analyzed with Randomise (part of FSL) to test for group differences between the patient and control groups. This program performed permutation-based testing with 5,000 permutations and statistical inference by using threshold-free cluster enhancement (TFCE) [22] with a threshold of P<0.05, corrected for multiple comparisons (family-wise error). Randomise was also used to examine the relationship between FA/MD/MK and disease duration, Hoehn–Yahr stage, and levodopa dosage in the PD patient group with multiple linear regression analysis (P<0.05, corrected for gender and age at the time of MRI). The anatomical locations of regions with significant group differences in FA and MD on the white matter skeleton were identified with a white matter atlas [23].

Analysis of crossing fibers

The superior longitudinal fasciculus (SLF) contains a relatively large number of voxels with multiple fiber orientations due to the crossing of the corona radiata, laterally projecting fibers of the corpus callosum, or both [30]. ROI analysis was performed for the area of the posterior corona radiata and SLF fiber crossing.

On the color maps, red, green, and blue were assigned to the left–right, antero-posterior, and cranio-caudal directions, respectively. The corona radiata are easily identified in blue owing to their predominantly cranio-caudal direction (Fig. 1a). Fibers of the SLF are identified in green owing to

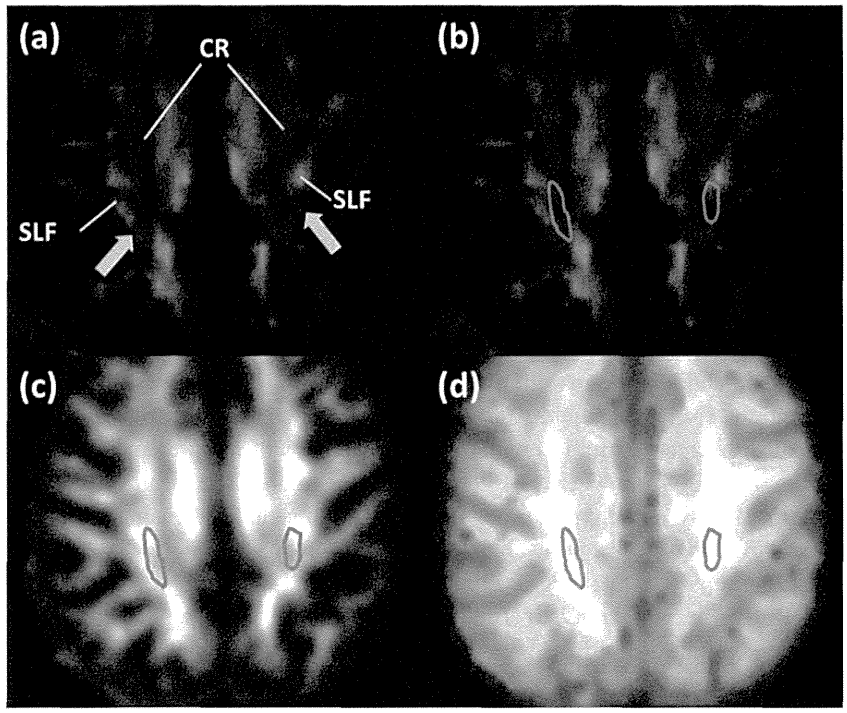

Fig. 1 Procedure used to draw regions of interest (ROI) on the area of the posterior corona radiata and crossing fibers of the superior longitudinal fasciculus (SLF). Axial color-coded fractional anisotropy (FA) maps (**a**, **b**) and an FA map (**c**) and corresponding and mean kurtosis (MK) map (**d**) depicting the superior longitudinal fasciculus (SLF) and posterior corona radiata (CR) are shown. **a** The CR were easily identified in *blue* on the color map owing to their predominantly cranio-caudal direction. The SLF was also identified in *green* on the color map owing to its predominantly antero-posterior orientation. In the area of the posterior corona radiata and SLF fiber crossing, *blue* (corona radiata) and *green* (SLF) are intermingled and the color becomes ambiguous (marked by *yellow arrows*). **b** On the color map, we identified the axial slice where the area of the posterior corona radiata and SLF fiber crossing became the largest. In this slice, we drew the ROI manually on the area of the posterior corona radiata and SLF fiber crossing (*blue line*). **c**, **d** We applied this ROI to the FA (**c**) and MK (**d**) maps of the same slice

their predominantly antero-posterior orientation (Fig. 1a). In the area of the posterior corona radiata and SLF fiber crossing, blue (corona radiata) and green (SLF) are intermingled and the color becomes ambiguous (Fig. 1a).

The following method was used to draw an ROI. First, on the color map, we identified the axial slice where the area of the posterior corona radiata and SLF fiber crossing was the largest (Fig. 1a). Second, in this slice, we drew the ROI manually on the area of the posterior corona radiata and SLF crossing fibers (Fig. 1b). We applied this ROI to FA and MK maps of the same slice (Fig. 1c, d). Both investigators agreed a priori upon the common method described above. All ROIs were drawn by individuals blind to the patient or control status.

Statistical analysis

All statistical analyses were performed with the Statistical Package for the Social Sciences for Windows, Release 20.0 (SPSS, Chicago, IL). Statistical analysis of demographic and clinical data was conducted with Student's t test for continuous variables and the χ^2 test for categorical data. The criterion of statistical significance was set to $P<0.05$. Student's t test was used to compare the averaged values of MD, FA, and MK for the area of the posterior corona radiata and SLF fiber crossing between PD patients and healthy controls. A Bonferroni correction was applied to the number of comparisons ($n=3$: [MD, FA, MK], setting the level of significance at $P<0.05/3=0.016$). Interrater reliability was assessed by using Pearson's correlation coefficient.

Results

Demographic and clinical features

Age ($P=0.82$, Student's t test) and sex distribution ($P=0.42$, χ^2) did not differ between PD patients and healthy controls (Table 1).

White matter alteration assessed with TBSS

FA values in the frontal white matter, part of the genu of the corpus callosum, and part of the parietal white matter were significantly lower in PD patients than in healthy controls. The affected white matter tracts included the anterior part of the

inferior fronto-occipital fasciculus (IFOF), anterior SLF, and anterior and superior corona radiata (i.e., the frontal white matter); in part of the posterior SLF and in part of the genu and body of the corpus callosum, FA values were significantly lower in controls than in PD patients (Fig. 2a).

Reductions in MK were seen more extensively throughout the brain: in addition to the frontal white matter, reduced MK was seen in the parietal, occipital, and right temporal white matter. The affected white matter tracts included the SLF and inferior longitudinal fasciculus; the IFOF; the uncinate fasciculus; and the anterior, posterior, and superior corona radiata (Fig. 2b). MD values were not significantly different in the cerebral white matter of PD patients compared with control subjects.

Analysis of crossing fibers

Compared with the area of parietal white matter in which FA was reduced, the MK reduction area was wider in range and included the area of the posterior corona radiata and SLF fiber crossing. In contrast to FA, MK is not limited to anisotropic environments; hence, it uniquely permits quantification of the microstructural integrity of white matter in the presence of crossing fibers. We hypothesized that the area of the posterior corona radiata and SLF fiber crossing influenced our TBSS results. We therefore compared diffusion abnormalities in the area of the posterior corona radiata and SLF fiber crossing in PD patients and normal controls by using an ROI analysis.

Reproducibility was expressed in terms of the interrater correlation coefficient; the coefficient in the posterior corona radiata crossing fibers of the SLF was 0.89 for the MD analysis. 0.84 for the FA analysis, and 0.95 for the MK analysis. Therefore, averaged values were used for subsequent statistical analyses.

FA and MD values were not significantly altered in the area of the posterior corona radiata and SLF fiber crossing in the PD group compared with the control group (MD: P=0.36, FA: P=0.95) (Table 2). Only MK values were reduced in the PD group compared with the control group (MK: P=0.001) (Table 2).

Discussion

Three findings were confirmed in this study. First, we demonstrated that FA values in the frontal white matter (anterior part of the IFOF, anterior SLF, and anterior and superior corona radiata), part of the genu and body of the corpus callosum, and part of the parietal white matter (in part of the posterior SLF) were significantly lower in PD patients than in healthy controls. Second, reductions in MK values occurred across a more extensive area than FA reduction: in addition to the frontal white matter, reduced MK values were seen in the parietal, occipital, and right temporal white matter. Third, the MK value of the area of the posterior corona radiata and SLF fiber crossing was reduced in the PD group compared with the control group. Although previous DKI studies of the basal ganglia and substantia nigra by Wang et al. [23] and of the cingulate fiber tracts by our group [24] have revealed changes in diffusion metrics specific to PD patients, to the best of our knowledge, the present study is the first to evaluate white matter by using whole-brain DKI analysis in PD patients.

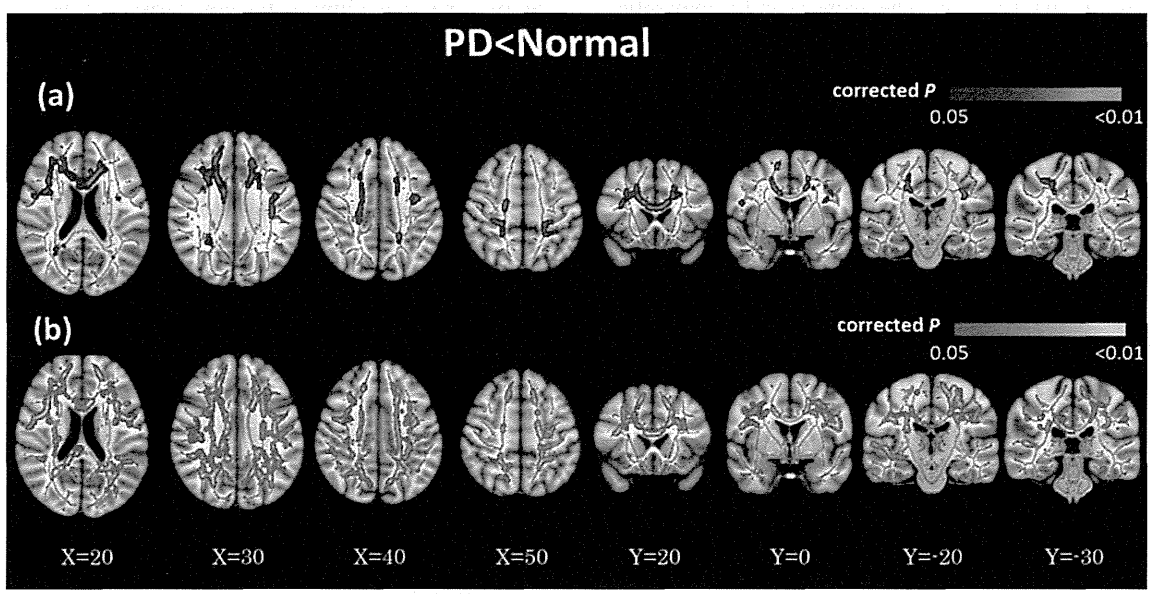

Fig. 2 Comparison of DTI and DKI metrics between PD patients and controls. TBSS maps of decreased FA (**a**) and decreased MK (**b**) in PD patients compared with age-matched healthy subjects shown in neurological convention. In the TBSS maps, the FA skeleton with FA >0.2 is shown in *green*, and voxels in which the one-sided permutation-corrected P was <0.05 are marked in *blue* (FA) or *red* (MK)

Table 2 Comparison of DT/DK parameters in the area of the posterior corona radiata and SLF fiber crossing

	CN	PD	PD − *N* (%)	*P* value
Area of the posterior corona radiata and SLF fiber crossing				
MK	1.15±0.06	1.04±0.06	−9.5	0.001[a]
FA	0.32±0.03	0.32±0.08	−2.8	0.95
MD	0.71±0.02	0.73±0.04	+2.1	0.36

Values are means ± SD. FA and MK are dimensionless. Mean diffusivity values are given in 1,000 mm^2/s. PD − *N* = (PD − *N*) / *N* × 100

CN healthy controls, *PD* Parkinson disease, *MK* mean kurtosis, *FA* fractional anisotropy, *MD* mean diffusivity

[a] Significant difference between groups

The reduced FA values in the frontal lobe of PD patients agree with the results of previous studies [9, 13–15]. According to the staging system proposed by Braak et al. [2, 4], neuropathological stages are divided into six subgroups depending on where Lewy bodies are deposited. In stages 1 and 2, Lewy-related inclusion bodies remain confined to the medulla oblongata and olfactory bulb. In stages 3 and 4, the substantia nigra and other nuclei of the midbrain and basal forebrain are the focus of initially subtle and later severe changes. In end stages 5 and 6, the pathological process encroaches upon the cerebral cortex. The deposition of Lewy bodies in the prefrontal area is classified as stage 5—a relatively early stage for the neocortex. Pathological changes in white matter in the form of Lewy neurites or pale neurites, which accumulate in brainstem axons and later spread to the cerebral white matter, are also found in parallel with Lewy bodies in PD [2, 4]. These accumulated Lewy pathologies may alter the axonal structure. The decrease in FA may reflect neuronal loss and reduced anisotropy due to the deposition of axonal Lewy neurites or pale neurites.

Currently, mainly the end phase of the pathologic process of PD can be detected clinically [2, 4]. In Braak staging, autopsy material from patients who manifest clinical findings consistent with PD can be assigned to one of three subgroups (stages 4–6) depending on the locations of Lewy deposits. In stage 6, Lewy-related pathology reaches the entire cerebrum; therefore, the extensive area across which MK was reduced may reflect white matter alteration caused by Lewy-related pathologies such as Lewy neurites or pale neurites.

Although traditional DTI assumes that water molecules display Gaussian diffusion in a hindered and unrestricted environment, in biological structures, they are restricted by cell membranes or organelles and thus often display non-Gaussian diffusion. Therefore, the sensitivity of DTI is limited by the diffusional and microstructural properties of biological structures [31]. Because kurtosis is a measure of the deviation of the diffusion profile from a Gaussian distribution, DKI quantifies the degree of diffusional non-Gaussianity or tissue complexity. Therefore, DKI would appear adequate for analyzing the structure of the human brain [31]. Our results suggest that the assessment of diffusional non-Gaussianity by using DKI may supply more sensitive metrics of changes in tissue microstructure than does traditional DTI.

DKI is also potentially useful for evaluating crossing fibers [32], whereas DTI metrics such as FA and MD in white matter are influenced by the presence of crossing fibers [33–35]. The adverse effects of crossing fibers on the interpretation of DTI metrics have been previously demonstrated [36, 37]. If two fiber populations are present within a voxel (crossing fiber), the shape of the diffusion tensor becomes more planar. Therefore, FA and MD values are lower in areas where fibers cross because of the lower directionality of diffusion on the voxel scale [36, 37]. As a result, the FA value of a voxel with intact crossing fibers can be similar to that of a voxel with a degenerating area with noncrossing fibers [30]. In our TBSS results, the area of MK reduction includes that of the posterior corona radiata and SLF crossing fibers, whereas no change in FA was observed in this area. Furthermore, a significant MK reduction in this area was also detected by ROI analysis, whereas no such change of MD or FA occurred in this area, confirming the robustness of our results. That DKI can identify areas of fiber crossing may be one reason why MK is sensitive to changes in cerebral white matter.

Our study has a number of limitations. First, because the PD diagnoses were not histopathologically confirmed, the possibility of misdiagnosis remains. However, the validity of the diagnoses is strengthened by the observation that, after being followed for 18 months, all patients continued to respond satisfactorily to antiparkinsonian therapy and remained free of atypical parkinsonisms. Second, the small size of our samples may have limited the comparison of disease severity and DT/DK parameters. Third, the ROIs on the area of the posterior corona radiata and SLF fiber crossing were drawn manually, and the reproducibility of measurements was unclear. However, all ROIs were drawn by two of the authors, rater bias was prevented by blinding, and the interclass correlation coefficients were 0.84–0.95.

Conclusion

DKI can detect cerebral white matter alteration in PD patients more sensitively than can conventional DTI. By providing a potentially more sensitive index of brain pathology in PD, DKI may enable improved monitoring of disease progression and more effective treatment planning.

Acknowledgments We thank Nozomi Hamasaki and Syuji Sato, MR imaging technologists, for their skillful performance in acquiring data; Akira Nishikori, Tomomi Okamura and Fumitaka Kumagai for their research assistance; and Yuriko Suzuki and Masaru Takashima, Philips

Healthcare, for their technical assistance. We also thank Narisumi Cho for administrative assistance. This work was supported by a Grant-in-Aid for Scientific Research on Innovative Areas (Comprehensive Brain Science Network) from the Ministry of Education, Culture, Sports, Science, and Technology of Japan and MEXT/JSPS KAKENHI grant number 24591787.

Conflict of interest We declare that we have no conflict of interest.

References

1. de Lau LM, Breteler MM (2006) Epidemiology of Parkinson's disease. Lancet Neurol 5(6):525–535. doi:10.1016/S1474-4422(06)70471-9
2. Braak H, Del Tredici K (2008) Invited article: nervous system pathology in sporadic Parkinson disease. Neurology 70(20):1916–1925. doi:10.1212/01.wnl.0000312279.49272.9f
3. Braak H, Del Tredici K, Bratzke H, Hamm-Clement J, Sandmann-Keil D, Rub U (2002) Staging of the intracerebral inclusion body pathology associated with idiopathic Parkinson's disease (preclinical and clinical stages). J Neurol 249(Suppl 3):III/1–III/5
4. Braak H, Del Tredici K, Rub U, de Vos RA, Jansen Steur EN, Braak E (2003) Staging of brain pathology related to sporadic Parkinson's disease. Neurobiol Aging 24(2):197–211
5. Braak H, Ghebremedhin E, Rub U, Bratzke H, Del Tredici K (2004) Stages in the development of Parkinson's disease-related pathology. Cell Tissue Res 318(1):121–134. doi:10.1007/s00441-004-0956-9
6. Braak H, Muller CM, Rub U, Ackermann H, Bratzke H, de Vos RA, Del Tredici K (2006) Pathology associated with sporadic Parkinson's disease—where does it end? J Neural Transm Suppl 70:89–97
7. Kamagata K, Motoi Y, Abe O, Shimoji K, Hori M, Nakanishi A, Sano T, Kuwatsuru R, Aoki S, Hattori N (2012) White matter alteration of the cingulum in Parkinson disease with and without dementia: evaluation by diffusion tensor tract-specific analysis. AJNR Am J Neuroradiol 33(5):890–895. doi:10.3174/ajnr.A2860
8. Kamagata K, Motoi Y, Hori M, Suzuki M, Nakanishi A, Shimoji K, Kyougoku S, Kuwatsuru R, Sasai K, Abe O, Mizuno Y, Aoki S, Hattori N (2011) Posterior hypoperfusion in Parkinson's disease with and without dementia measured with arterial spin labeling MRI. J Magn Reson Imaging JMRI 33(4):803–807. doi:10.1002/jmri.22515
9. Karagulle Kendi AT, Lehericy S, Luciana M, Ugurbil K, Tuite P (2008) Altered diffusion in the frontal lobe in Parkinson disease. AJNR Am J Neuroradiol 29(3):501–505. doi:10.3174/ajnr.A0850
10. Lee JE, Park HJ, Park B, Song SK, Sohn YH, Lee JD, Lee PH (2010) A comparative analysis of cognitive profiles and white-matter alterations using voxel-based diffusion tensor imaging between patients with Parkinson's disease dementia and dementia with Lewy bodies. J Neurol Neurosurg Psychiatry 81(3):320–326. doi:10.1136/jnnp.2009.184747
11. Vaillancourt DE, Spraker MB, Prodoehl J, Abraham I, Corcos DM, Zhou XJ, Comella CL, Little DM (2009) High-resolution diffusion tensor imaging in the substantia nigra of de novo Parkinson disease. Neurology 72(16):1378–1384. doi:10.1212/01.wnl.0000340982.01727.6e
12. Hattori T, Orimo S, Aoki S, Ito K, Abe O, Amano A, Sato R, Sakai K, Mizusawa H (2012) Cognitive status correlates with white matter alteration in Parkinson's disease. Hum Brain Mapp 33(3):727–739. doi:10.1002/hbm.21245
13. Matsui H, Nishinaka K, Oda M, Niikawa H, Kubori T, Udaka F (2007) Dementia in Parkinson's disease: diffusion tensor imaging. Acta Neurol Scand 116(3):177–181. doi:10.1111/j.1600-0404.2007.00838.x
14. Zhan W, Kang GA, Glass GA, Zhang Y, Shirley C, Millin R, Possin KL, Nezamzadeh M, Weiner MW, Marks WJ Jr, Schuff N (2012) Regional alterations of brain microstructure in Parkinson's disease using diffusion tensor imaging. Mov Disord Off J Mov Disord Soc 27(1):90–97. doi:10.1002/mds.23917
15. Zhang K, Yu C, Zhang Y, Wu X, Zhu C, Chan P, Li K (2011) Voxel-based analysis of diffusion tensor indices in the brain in patients with Parkinson's disease. Eur J Radiol 77(2):269–273. doi:10.1016/j.ejrad.2009.07.032
16. Haller S, Badoud S, Nguyen D, Garibotto V, Lovblad KO, Burkhard PR (2012) Individual detection of patients with Parkinson disease using support vector machine analysis of diffusion tensor imaging data: initial results. AJNR Am J Neuroradiol 33(11):2123–2128. doi:10.3174/ajnr.A3126
17. Basser PJ, Jones DK (2002) Diffusion-tensor MRI: theory, experimental design and data analysis—a technical review. NMR Biomed 15(7–8):456–467. doi:10.1002/nbm.783
18. Hui ES, Cheung MM, Qi L, Wu EX (2008) Towards better MR characterization of neural tissues using directional diffusion kurtosis analysis. Neuroimage 42(1):122–134. doi:10.1016/j.neuroimage.2008.04.237
19. Jensen JH, Helpern JA, Ramani A, Lu H, Kaczynski K (2005) Diffusional kurtosis imaging: the quantification of non-Gaussian water diffusion by means of magnetic resonance imaging. Magn Reson Med Off J Soc Magn Reson Med Soc Magn Reson Med 53(6):1432–1440. doi:10.1002/mrm.20508
20. Lu H, Jensen JH, Ramani A, Helpern JA (2006) Three-dimensional characterization of non-Gaussian water diffusion in humans using diffusion kurtosis imaging. NMR Biomed 19(2):236–247. doi:10.1002/nbm.1020
21. Jensen JH HJ (2003a) Quantifying non-Gaussian water diffusion by means of pulsed-field-gradient MRI. Presented at the International Society for Magnetic Resonance in Medicine annual meeting, Toronto, Canada 11:2154
22. Jensen JH, Helpern JA (2010) MRI quantification of non-Gaussian water diffusion by kurtosis analysis. NMR Biomed 23(7):698–710. doi:10.1002/nbm.1518
23. Wang JJ, Lin WY, Lu CS, Weng YH, Ng SH, Wang CH, Liu HL, Hsieh RH, Wan YL, Wai YY (2011) Parkinson disease: diagnostic utility of diffusion kurtosis imaging. Radiology 261(1):210–217. doi:10.1148/radiol.11102277
24. Kamagata K, Tomiyama H, Motoi Y, Kano M, Abe O, Ito K, Shimoji K, Suzuki M, Hori M, Nakanishi A, Kuwatsuru R, Sasai K, Aoki S, Hattori N (2013) Diffusional kurtosis imaging of cingulate fibers in Parkinson disease: comparison with conventional diffusion tensor imaging. Magn Reson Imaging 31(9):1501–1506. doi:10.1016/j.mri.2013.06.009
25. Smith SM, Jenkinson M, Johansen-Berg H, Rueckert D, Nichols TE, Mackay CE, Watkins KE, Ciccarelli O, Cader MZ, Matthews PM, Behrens TE (2006) Tract-based spatial statistics: voxelwise analysis of multi-subject diffusion data. Neuroimage 31(4):1487–1505. doi:10.1016/j.neuroimage.2006.02.024
26. Kubicki M, Westin CF, Maier SE, Frumin M, Nestor PG, Salisbury DF, Kikinis R, Jolesz FA, McCarley RW, Shenton ME (2002) Uncinate fasciculus findings in schizophrenia: a magnetic resonance diffusion tensor imaging study. AJ Psychiatry 159(5):813–820
27. Kunimatsu A, Aoki S, Masutani Y, Abe O, Mori H, Ohtomo K (2003) Three-dimensional white matter tractography by diffusion tensor imaging in ischaemic stroke involving the corticospinal tract. Neuroradiology 45(8):532–535. doi:10.1007/s00234-003-0974-4
28. Hori M, Fukunaga I, Masutani Y, Nakanishi A, Shimoji K, Kamagata K, Asahi K, Hamasaki N, Suzuki Y, Aoki S (2012) New diffusion metrics for spondylotic myelopathy at an early clinical stage. Eur Radiol 22(8):1797–1802. doi:10.1007/s00330-012-2410-9
29. Jenkinson M, Bannister P, Brady M, Smith S (2002) Improved optimization for the robust and accurate linear registration and motion correction of brain images. Neuroimage 17(2):825–841